Distinctive Skeletal Phenotype in High Bone Mass Osteogenesis Imperfecta Due to a *COL1A2* Cleavage Site Mutation

Gen Nishimura,[1]* **Masahiro Nakajima,**[2] **Kazuharu Takikawa,**[3] **Nobuhiko Haga,**[4] **and Shiro Ikegawa**[2]

[1]Department of Pediatric Imaging, Tokyo Metropolitan Children's Medical Center, Tokyo, Japan

[2]Laboratory for Bone and Joint Diseases, RIKEN Center for Integrative Medical Sciences, Tokyo, Japan

[3]Department of Orthopedics, Shizuoka Children's Hospital, Shizuoka, Japan

[4]Department of Rehabilitation Medicine, University of Tokyo, Tokyo, Japan

TO THE EDITOR:

Over 15 years ago, we encountered a family (six affected individuals) with a fragile bone disease inherited as an autosomal dominant trait. We reported the family as having a "new brittle bone disorder" in AJMG [Nishimura et al., 1999]. At that time, we presumed that the disorder differed from osteogenesis imperfecta (OI), because the clinical hallmark was bent bones rather than fractures.

We recently performed molecular analyses for the family (the proband, affected mother, and healthy father). After informed

consent, the DNAs of the family members were obtained. Whole exome sequencing revealed a novel C-propeptide cleavage site mutation in *COL1A2* (c.3358G>A, p.Asp1120Asn) in the proband and affected mother, which was confirmed by subsequent Sanger sequencing (Fig. 1). We report here on the recent skeletal phenotype of the proband, and also discuss the radiological characteristics of patients with mutations that impair C-propeptide cleavage of type 1 procollagen.

As we previously reported, the phenotypic variations in this family were remarkable. Affected family members had varying degrees of bone fragility and abnormal bone mineralization. The proband was a boy who was most severely affected in this family. He presented with progressive symmetric bowing of the forearms and legs despite only a few episodes of fractures. The distal femora and distal ulnae showed sharp angular deformities associated
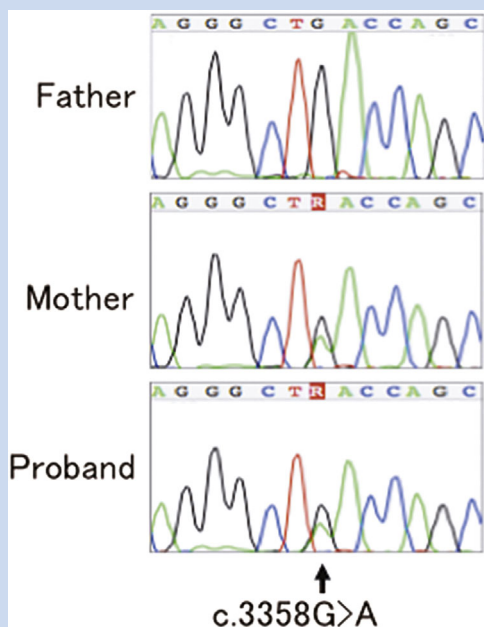
FIG. 1. Sanger sequencing for the novel C-propeptide cleavage site mutation of *COL1A2* (c.3358G>A) in the family. [Color figure can be seen in the online version of this article, available at http://wileyonlinelibrary.com/journal/ajmga].

with pseudo-fractures, the proximal fibulae were attenuated, and the right fibula showed a pseudo-fracture (Fig. 1A and B). The distal ulnae showed progressive shortening and constriction with increasing age. The bone trabecular pattern appeared coarse. He underwent corrective surgery for his leg and forearm deformities on a few occasions. His male cousin also had symmetric bowing of the forearms. Other affected individuals had very few or no fractures; yet, they all showed a coarse bone trabecular pattern.

At the last visit, the proband was 28 years old. No fracture occurred after adolescence. He never received bisphosphonate therapy. Height was 149.3 cm (−3.7 SD) and weight 57.9 kg (−0.5 SD). He presented with genu valgus deformities with patellar dislocation. The knee joints were sometimes painful, and knee flexion was mildly restricted. Forearm movement was mildly restricted as well. Radiological examination at age 19 years and 27 years displayed severe valgus deformities of the knee and irregular contours of the femora, tibiae and fibulae. The radii and ulnae were bowed, the proximal radii were dislocated, the distal ulnae were attenuated, and the proximal ulnae were mildly thickened. The radioulnar interosseous membranes exhibited mild ossification (Fig. 2). Radio-

graphically the bone appeared dense, but unfortunately skeletal densitometry was not performed.

Recent investigations on OI have demonstrated that mono-allelic C-propeptide cleavage site mutations in *COL1A1* and *COL1A2* and bi-allelic mutations in *BMP1* (the gene encoding a C-propetide cleavage enzyme) constitute a distinctive subgroup of OI. These mutations interfere with the removal of the global C-terminal propeptide from the type 1 pro-collagen chain in the endoplasmic reticulum, and cause incorporation of uncleaved C-propeptides into the extracellular matrices. The morphological consequences include increased osteoid and high bone mineral density; thus the phenotype is termed "high bone mass OI" [Lindahl et al., 2011; Asharani et al., 2012; Hoyer-Kuhn et al., 2013]. The pathogenesis of the increased osteoid and increased mineralization remains elusive; however, it is assumed that the former is attributed to delayed maturation of osteoid, while the latter is due to abundant mineralization in mature osteoid [Hoyer-Kuhn et al., 2013]. Osteoclastic activities are increased as well [Hoyer-Kuhn et al., 2013; Asharani et al., 2012]. Similarly, double knock-out mice of *Bmp1* and *Tll1* (another propeptide cleaving enzyme) show not only bone fragility but also histological evidence increased osteoid seams [Muir et al., 2014].
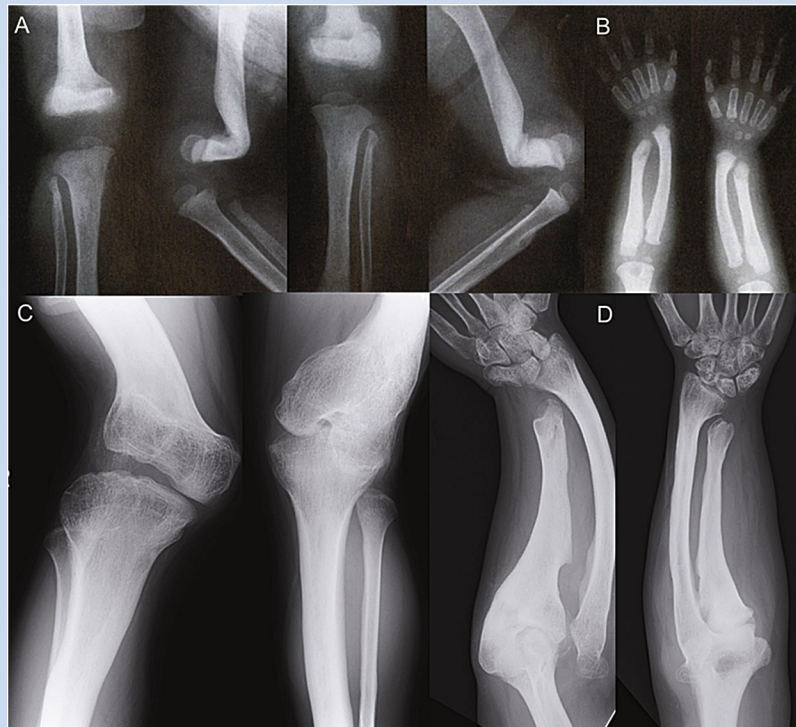

FIG. 2. A: Radiographs of the knees at age 22 months: the distal femora show sharp posterior angulation. The proximal fibulae are constricted. A pseudo-fracture is noted in the right proximal fibula. **B:** Radiographs of the forearms at age 3 3/12 years: The radii and ulnae are mildly bowed. The distal ulnae are constricted along with pseudo-fractures. **C:** Radiographs of the knees at age 19 years: Valgus deformity is remarkable. Irregular contours are seen in the left femur and right tibia. **D:** Radiographs of the forearms at age 27 years: The radii and ulnae are bowed, and the proximal radii are dislocated. The distal ulnae are narrow, while the proximal ulnae appear mildly thick. Mild ossification is seen in the radioulnar interosseous membranes. A and B are reproduced from AJMG 84:320–329 (1999) by permission of the publisher.

In the high bone mass OI, osteosclerosis is progressive with age, and may not be easily identifiable in younger patients. In the present patient, osteosclerosis did not initially come to our attention. In retrospect, however, sclerotic changes were discernible in the long bones, particularly the femora, radii and ulnae. His recent radiographs demonstrated more clearly the presence of osteosclerosis in the long bones (Fig. 2). His other skeletal hallmarks, including coarse trabeculae, pseudo-fractures, and metaphyseal constriction are quite similar to those of patients with *BMP1* mutations [Asharani et al., 2012; Cho et al., 2015]. Thus, these skeletal changes are likely to be an essential component in the high bone mass OI, which are probably related to hyper-osteoidosis (increased osteoid) and/or increased osteoclastic activity.

From the clinical viewpoint, the high bone mass OI belongs to a benign form of OI spectrum [Lindahl et al., 2011; Asharani et al., 2012; Hoyer-Kuhn et al., 2013]. Fractures are not so frequent, deformities are not severely progressive, blue sclera and dentinogenesis imperfecta are absent, and short stature absent or mild, as was seen in the present patient. The benign clinical course is quite different from severe or lethal outcome in the other subset of dense bone OI due to C-propeptide mutations at the non-cleavage site [Pace et al., 2002; Takagi et al., 2011].

In conclusion, a phenotypically distinctive group of OI is caused by a mono-allelic *COL1* C-propeptide cleavage site mutations and biallelic *BMP1* mutations. The subgroup is characterized by high bone mass and other unique skeletal changes, such as coarse trabeculae, pseudo-fractures, and metaphyseal constriction.

ACKNOWLEDGMENT

REFERENCES

Asharani PV, Keupp K, Semler O, Wang W, Li Y, Thiele H, Yigit G, Pohl E, Becker J, Frommolt P, Sonntag C, Altmüller J, Zimmermann K, Greenspan DS, Akarsu NA, Netzer C, Schönau E, Wirth R, Hammerschmidt M, Nürnberg P, Wollnik B, Carney TJ. 2012. Attenuated BMP1 function compromises osteogenesis, leading to bone fragility in humans and zebrafish. Am J Hum Genet 90:661–674.

Cho SY, Asharani PV, Kim OH, Iida A, Miyake N, Matsumoto N, Nishimura G, Ki CS, Hong G, Kim SJ, Sohn YB, Park SW, Lee J, Kwun Y, Carney TJ, Huh R, Ikegawa S, Jin DK. 2015. Identification and in vivo functional characterization of novel compound heterozygous BMP1 variants in osteogenesis imperfecta. Hum Mutat 36:191–195.

Hoyer-Kuhn H, Semler O, Schoenau E, Roschger P, Klaushofer K, Rauch F. 2013. Hyperosteoidosis and hypermineralization in the same bone: Bone tissue analyses in a boy with a homozygous BMP1 mutation. Calcif Tissue Int 93:565–570.

Lindahl K, Barnes AM, Fratzl-Zelman N, Whyte MP, Hefferan TE, Makareeva E, Brusel M, Yaszemski MJ, Rubin CJ, Kindmark A, Roschger P, Klaushofer K, McAlister WH, Mumm S, Leikin S, Kessler E, Boskey AL, Ljunggren O, Marini JC. 2011. COL1 C-propeptide cleavage site mutations cause high bone mass osteogenesis imperfecta. Hum Mutat 32:598–609.

Muir AM, Ren Y, Butz DH, Davis NA, Blank RD, Birk DE, Lee SJ, Rowe D, Feng JQ, Greenspan DS. 2014. Induced ablation of Bmp1 and Tll1 produces osteogenesis imperfecta in mice. Hum Mol Genet 23:3085–3101.

Nishimura G, Haga N, Aoki K, Hamazaki M, Taniguchi K, Iwaya T. 1999. New brittle bone disorder: Report of a family with six affected individuals. Am J Med Genet 84:320–329.

Pace JM, Chitayat D, Atkinson M, Wilcox WR, Schwarze U, Byers PH. 2002. A single amino acid substitution (D1441Y) in the carboxyl-terminal propeptide of the proalpha1(I) chain of type I collagen results in a lethal variant of osteogenesis imperfecta with features of dense bone diseases. J Med Genet 39:23–29.

Takagi M, Hori N, Chinen Y, Kurosawa K, Tanaka Y, Oku K, Sakata H, Fukuzawa R, Nishimura G, Spranger J, Hasegawa T. 2011. Heterozygous C-propeptide mutations in COL1A1: Osteogenesis imperfecta type IIC and dense bone variant. Am J Med Genet Part A 155A:2269–2273.

Reactivation of epigenetically silenced miR-124 reverses the epithelial-to-mesenchymal transition and inhibits invasion in endometrial cancer cells via the direct repression of IQGAP1 expression

Peixin Dong[1,*], Kei Ihira[2,*], Ying Xiong[3,*], Hidemichi Watari[2], Sharon J.B. Hanley[1], Takahiro Yamada[1], Masayoshi Hosaka[2], Masataka Kudo[2], Junming Yue[4,5], Noriaki Sakuragi[1,2]

[1]Department of Women's Health Educational System, Hokkaido University School of Medicine, Hokkaido University, N15, W7, Sapporo, Japan

[2]Department of Gynecology, Hokkaido University School of Medicine, Hokkaido University, N15, W7, Sapporo, Japan

[3]Department of Gynecology, State Key Laboratory of Oncology in South China, Sun Yat-sen University Cancer Center, Guangzhou, P. R. China

[4]Department of Pathology and Laboratory Medicine, University of Tennessee Health Science Center, TN, USA

[5]Center for Cancer Research, University of Tennessee Health Science Center, Memphis, TN, USA

[*]These authors have contributed equally to this work

Correspondence to: Peixin Dong, email: dpx1cn@gmail.com
Hidemichi Watari, email: watarih@med.hokudai.ac.jp
Junming Yue, email: jyue@uthsc.edu

ABSTRACT

Overexpression of IQGAP1 and microRNA (miRNA) dysregulation are frequent in human tumors, but little is known about the role of IQGAP1 and its relationship to miRNA in endometrial carcinogenesis. We demonstrate that IQGAP1 activates the epithelial–mesenchymal transition (EMT) program and that miR-124 directly represses IQGAP1 expression in endometrial cancer (EC) cells. The overexpression of IQGAP1 stimulates EMT features and enhances migration, invasion and proliferation of EC cells, whereas knocking down IQGAP1 expression reverses EMT and inhibits these malignant properties. Using miRNA microarray profiling, we identified 29 miRNAs (let-7b, let-7f, miR-10b, miR-15b, miR-23a, miR-24, miR-25, miR-27a, miR-29b, miR-30a-5p, miR-34a, miR-124, miR-127, miR-130b, miR-148a, miR-155, miR-191*, miR-194, miR-224, miR-362, miR-409-3p, miR-422b, miR-424, miR-453, miR-497, miR-518d, miR-518f*, miR-526a and miR-656) that are significantly down-regulated in an *in vitro*-selected highly invasive derivative cell line (HEC-50-HI) relative to the parental HEC-50 cells. We further identified miR-124 as a direct regulator of IQGAP1 in EC cells. Enforced expression of miR-124 suppresses EC cell invasion and proliferation. The expression of IQGAP1 mRNA was significantly elevated in EC tissues, while the expression of miR-124 was decreased. The downregulation of miR-124 correlates with a poor survival outcome for patients with EC. Treating EC cells with the demethylating agent 5-aza-2'-deoxycytidine increased miR-124 expression and down-regulated IQGAP1 levels. Our data suggest that IQGAP1 promotes EMT, migration and invasion of EC cells. MiR-124, a novel tumor suppressor miRNA that is epigenetically silenced in EC, can reverse EMT and the invasive properties, by attenuating the expression of the *IQGAP1* oncogene.

BACKGROUND

The epithelial–mesenchymal transition (EMT), in which polarized epithelial cells become mesenchymal-migrating cells [1], is a key step promoting endometrial cancer (EC) metastasis [2, 3, 4]. IQGAP1 (IQ Motif Containing GTPase Activating Protein 1) is a scaffold protein that directly promotes actin polymerization by binding to F-actin [5], or indirectly modulates the cytoskeleton via interactions with the small GTPases Cdc42 and Rac1 [6]. IQGAP1 is overexpressed in different tumors other than EC, and its upregulation positively correlates with tumor metastasis [7, 8, 9, 10]. IQGAP1 also down-regulates E-cadherin, thereby attenuating cell–cell adhesions and promoting tumor cell invasion [11, 12]. Knocking down IQGAP1 impairs tumor cell growth, migration and invasion and the reversal of the EMT program [13], indicating that IQGAP1 expression is important for the induction of EMT. However, little is known about IQGAP1's expression, biological function and underlying regulatory mechanisms in EC.

MicroRNAs (miRNAs) are small RNA molecules that regulate EMT and metastasis [14]. Other epigenetic mechanisms, such as DNA methylation and histone modification, are critical for the regulation of EMT and miRNA expression in human cancer [15]. DNA methylation-based silencing of tumor suppressive miRNAs, such as miR-34b [16] and miR-124 [17], occurs in various human cancers and stimulates metastasis. IGGAP1 is targeted by miR-124 [18] in hepatocellular carcinoma and by miR-506 in breast cancer [19]. Nevertheless, the contribution of miRNAs to the regulation of IQGAP1 expression in EC is poorly understood.

Here, we provided the first evidence that IQGAP1 functions to promote EMT and invasion in EC cells. Moreover, we uncovered a novel mechanism by which the DNA methylation-associated silence of tumor suppressor miR-124 contributes to the upregulation of IQGAP1, suggesting that targeting the miR-124-IQGAP1 axis may have therapeutic potential for the treatment of invasive ECs.

RESULTS

IQGAP1 induces EMT, invasiveness and the proliferation of EC cells

Highly invasive subpopulations of HEC-50 cells were previously selected by using a transwell system to create the HEC-50-HI (HI) cell line [3]. We used real-time quantitative, reverse transcription-PCR (qPCR) to gain insight into the roles of IQGAP1 in EC and sought to determine its expression in the immortalized human endometrial epithelial (EM) cells and in three EC cells (HEC-1, HEC-50 and HI). The IQGAP1 mRNA was found to be markedly upregulated in EC cells relative to EM cells (Figure 1A), and its expression level was 3-fold higher in aggressive HI cells than in HEC-1 cells, which have a relatively lower metastatic potential (Figure 1B). This correlation suggests that IQGAP1 might play a role in EC metastasis.

To address this possibility, we used small-interference RNA (siRNA) to transiently knock down IQGAP1 expression in HI cells (Figure 1C) and observed a transition from a mesenchymal morphology to a more epithelial-like shape (Figure 1D), which was accompanied by the loss of N-cadherin expression and gain of E-cadherin expression (Figure 1C). To test whether IQGAP1 could induce the EMT program, we further transiently overexpress IQGAP1 in HEC-1 cells (Figure 1E). The ectopic expression of IQGAP1 promoted a mesenchymal morphology (Figure 1F) and resulted in increased N-cadherin and decreased E-cadherin expression (Figure 1E). These data suggest that the IQGAP1 levels are critical for the induction of EMT in EC cells.

To evaluate whether IQGAP1 could modulate the metastatic behavior of EC cells, we performed *in vitro* cell migration, invasion and proliferation assays after the knockdown or overexpression of IQGAP1. Silencing IQGAP1 in HI cells caused a significant decrease in the cell migration, invasion and proliferation, while elevating IQGAP1 expression significantly promoted these characteristics (Figure 1G, 1H, 1I, 1L). At the mRNA level, the qPCR analysis showed that downregulating IQPAP1 in HI cells increased the expression of epithelial markers *ZO-1* and *CK-18*, but reduced the expression of the mesenchymal marker *Vimentin* (Figure 1J). In contrast, the ectopic expression of IQGAP1 in HEC-1 cells activated *Vimentin* expression and inhibited *ZO-1* and *CK-18* levels (Figure 1K). This suggests that IQGAP1 induces mesenchymal-like phenotypes and enhances the mobility, invasion and proliferation of EC cells *in vitro*.

MiR-124 is down-regulated in highly invasive EC cells and directly suppresses IQGAP1 expression

To define the miRNAs that regulate IQGAP1 expression, we profiled the invasive HI and their parental HEC-50 cells using microarray analysis, and identified 29 miRNAs (let-7b, let-7f, miR-10b, miR-15b, miR-23a, miR-24, miR-25, miR-27a, miR-29b, miR-30a-5p, miR-34a, miR-124, miR-127, miR-130b, miR-148a, miR-155, miR-191*, miR-194, miR-224, miR-362, miR-409-3p, miR-422b, miR-424, miR-453, miR-497, miR-518d, miR-518f*, miR-526a and miR-656) that are significantly down-regulated in HI cells compared to HEC-50 cells (Figure 2A). Using qPCR, we validated the down-regulation of these 29 miRNAs in invasive HI cells versus their parental HEC-50 cells (data not shown). Of these miRNAs, we chose to focus on miR-124 because the computational target prediction using TargetScan predicted the presence of two conserved miR-124 seed-matching sequences

within the 3' untranslated region (3'-UTR) of *IQGAP1* mRNA (Figure 2B). To elucidate the relationship between miR-124 and IQGAP1 expression, we examined the expression of miR-124 in different EC cells and found the lowest levels of miR-124 in the highly invasive HI cells (Figure 2C), suggesting that reduced levels of miR-124 cause a dysregulation of IQGAP1 expression. Our qPCR and western blot analyses showed that increasing miR-124 levels in HI cells with the miR-124 mimic

reduced IQGAP1 expression, whereas inhibiting miR-124 by means of an anti-miR-124 inhibitor in HEC-1 cells increased IQGAP1 expression (Figure 2D, 2E). In another cellular context, we verified the inhibitory effects of miR-124 on IQGAP1 mRNA expression in human cervical cancer cells (HeLa cells; data not shown). Using a dual-reporter luciferase assay to investigate whether IQGAP1 is directly targeted by miR-124, we found that the IQGAP1 3'-UTR reporter activity was decreased by a miR-124

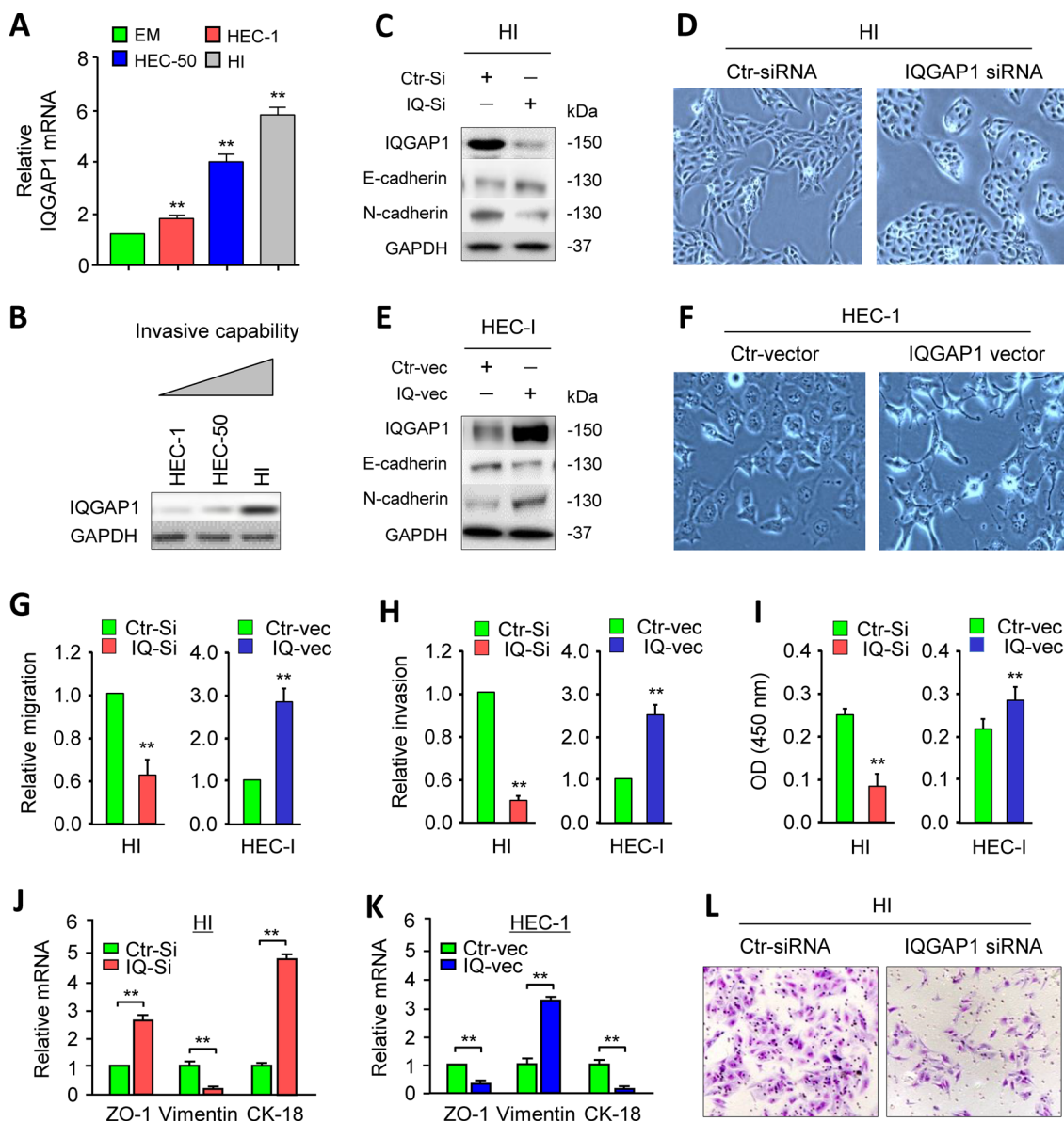**Figure 1: IQGAP1 induces the epithelial-to-mesenchymal transition, invasiveness, and proliferation of endometrial cancer (EC) cells. A.** Reverse transcription quantitative PCR (qPCR) analysis of IQGAP1 mRNA in the immortalized human endometrial cell line EM and the EC cells HEC-1, HEC-50, and HEC-50-HI (HI). The results are presented as the fold-change in expression compared to the EM cells. **B.** Western blot analysis of the IQGAP1 protein in EC cells. **C, E.** The expression of IQGAP1, E-cadherin, and N-cadherin proteins in HI cells transfected with control (Ctr) or IQGAP1 siRNA (C) and in HEC-1 cells expressing either the control or IQGAP1 vector (E). **D, F.** Phase-contrast microscopy shows the morphology of HI cells transfected with control or IQGAP1 siRNA (D) and HEC-1 cells transfected with the control or IQGAP1 vector (F). **G-I.** Detection of migration (G), invasion (H), and proliferation (I) in HI and HEC-1 cells after the indicated transfection. **J, K.** qPCR analysis of *ZO-1*, *CK-18*, and *Vimentin* expression in HI (J) and HEC-1 (K) cells, transfected as indicated. **L.** Representative images from the invasion assays.

mimic and increased by the anti-miR-124 inhibitor when the wild-type IQGAP1 3'-UTR was present. However, mutating the miR-124 binding sites in the IQGAP1 3'-UTR completely abrogated these effects (Figure 2F, 2G). Taken together, we showed that the *IQGAP1* mRNA is directly regulated by miR-124 via conserved seed-matching sequences.

MiR-124 maintains epithelial-like phenotypes and represses cell migration, invasion and proliferation in EC cells

To determine whether miR-124 inhibits EMT, we evaluated the effects of miR-124 overexpression on the cell morphology and invasion properties. Ectopically
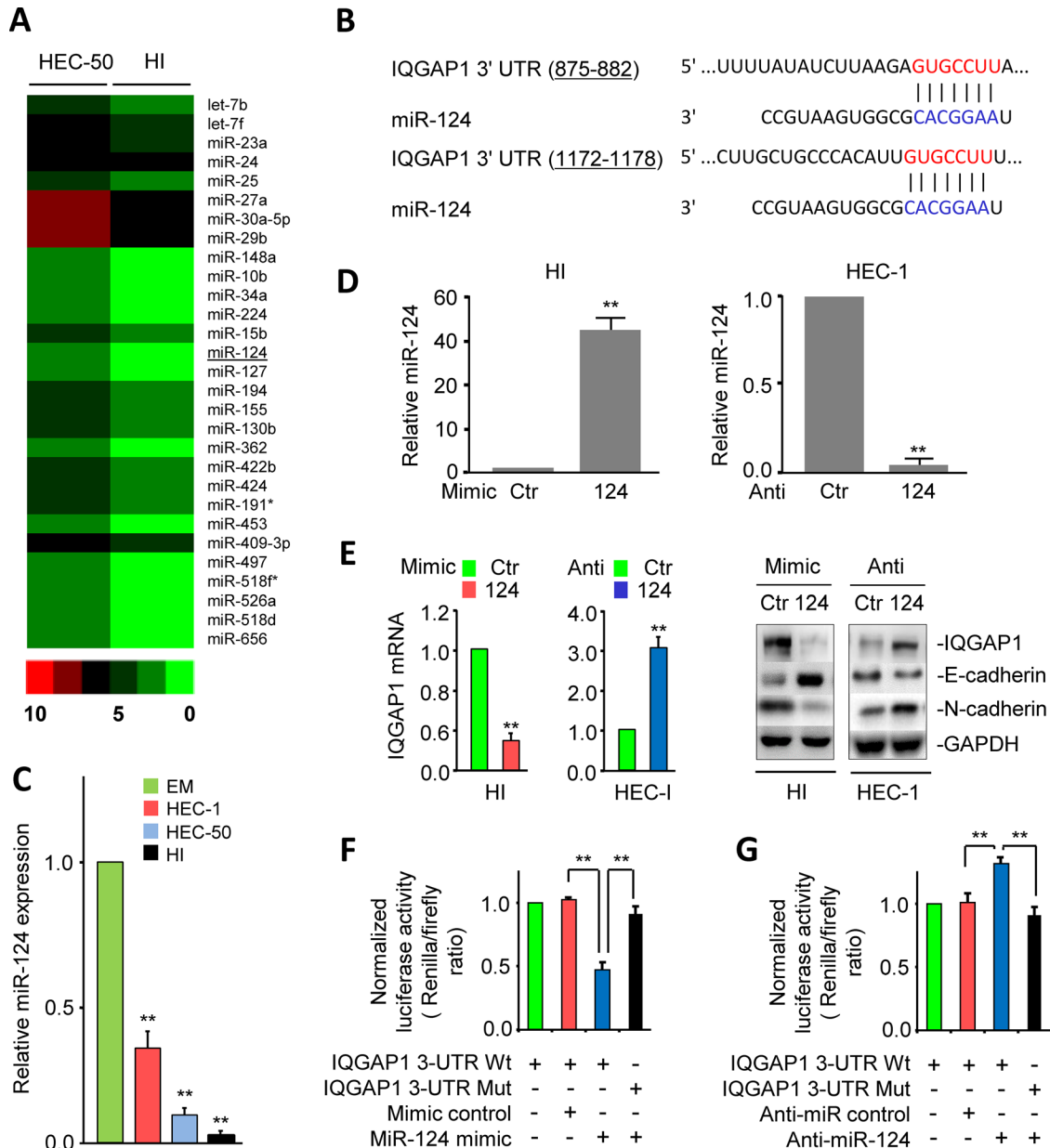

Figure 2: MiR-124 is down-regulated in highly invasive endometrial cancer (EC) cells and directly suppresses IQGAP1 expression. A. Profiling data of down-regulated microRNAs in highly invasive HEC-50-HI (HI) cells. **B.** Two putative conserved miR-124-binding sites in the *IQGAP1* 3' untranslated region (3'-UTR). **C.** Relative expression of miR-124 in immortalized human endometrial epithelial and EC cells, assessed by quantitative PCR assays. **D.** Expression of miR-124 in HI or HEC-1 cells transfected with a miR-124 mimic, miR-124 inhibitor, or their respective negative controls. **E.** Expression of the indicated mRNA and proteins in HI and HEC-1 cells after the overexpression or knockdown of miR-124. **F, G.** HI (F) and HEC-1 (G) cells were cotransfected with reporter plasmids containing wild-type *IQGAP1* or a mutant *IQGAP1* 3'-UTR together with a miR-124 mimic, miR-124 inhibitor, or respective negative control. The relative luciferase activity was assayed.

expressing miR-124 in HI cells resulted in the occurrence of epithelial morphology (Figure 3A). In contrast, down-regulating of endogenous miR-124 in HEC-1 cells produced a spindle-like morphology (Figure 3B). Cell migration, invasion and proliferation assays demonstrated that miR-124 inhibited the migration, invasion and proliferation of EC cells (Figure 3C, 3D, 3E). Conversely, the loss of miR-124 promoted these malignant features (Figure 3C, 3D, 3E). Furthermore, Western blot and qPCR analyses confirmed that in EC cells, forced expression of miR-124 significantly up-regulated the epithelial markers

(E-cadherin, *ZO-1* and *CK-18*), and down-regulated the mesenchymal markers (N-cadherin and *Vimentin*) in EC cells (Figure 2E; Figure 3F, 3G). To examine whether miR-124 suppress oncogenic phenotypes in HI cells through directly down-regulating IQGAP1, we performed the rescue experiments by overexpressing IQGAP1 in HI cells transfected with the miR-124 or a control mimic. Overexpression of IQGAP1 cDNA lacking the 3'-UTR sequence partially restored HI cell migration, invasion and proliferation reduced by miR-124 (Figure 3H, 3I and 3J). These results suggest that miR-124
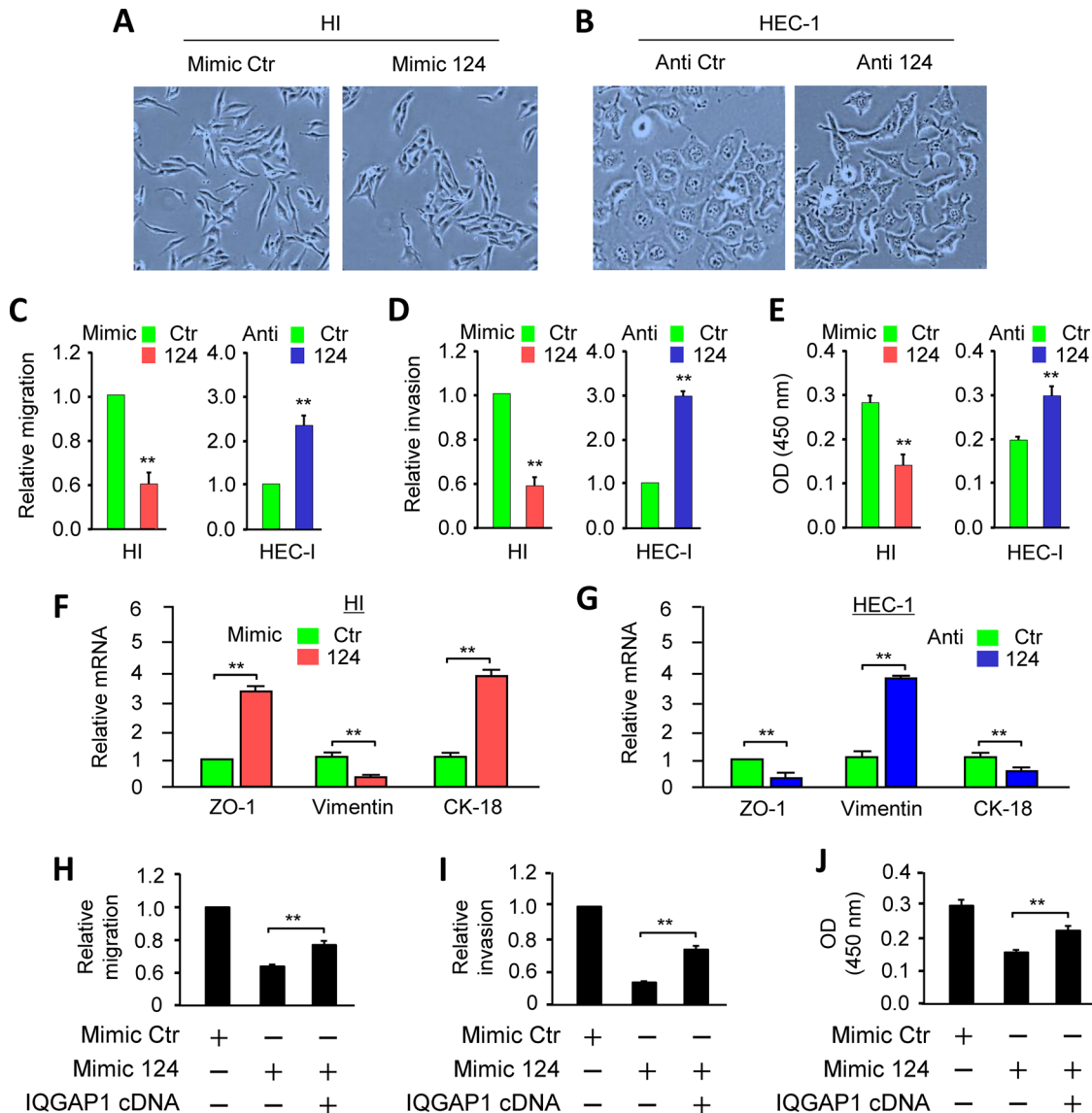

Figure 3: MiR-124 maintains epithelial-like phenotypes and represses cell migration, invasion, and proliferation in endometrial cancer cells. A. Overexpression of miR-124 in HEC-50-HI (HI) cells with fibroblastic morphology converts them to an epithelial-like morphology. **B.** HEC-1 cells transfected with miR-124 inhibitor exhibit more mesenchymal morphology than the control cells. (A and B, phase-contrast microscopy). **C-E.** Migration (C), invasion (D), and proliferation (E) of HI and HEC-1 cells after the overexpression or knockdown of miR-124. **F, G.** Quantitative PCR analysis of the indicated genes in HI (F) and HEC-1 (G) cells after the overexpression or knockdown of miR-124, as indicated. **H-J.** A miR-124 mimic or its control was transfected into HI cells along with a control vector or the IQGAP1 cDNA vector lacking the 3'-UTR region. The cells were assayed for cell migration (H), invasion (I), and proliferation (J). $^{**}P < 0.01$.

induces epithelial-like phenotypes, and also indicate that the repression of IQGAP1 by miR-124 represents an important mechanism by which miR-124 suppresses migration, invasion and proliferation.

Down-regulation of miR-124 is associated with elevated IQGAP1 expression in ECs

To test whether miR-124/IQGAP1 axis is clinically relevant in EC, we examined tumor specimens and adjacent normal tissues from 20 EC patients. Indeed, the qPCR analysis revealed a negative association between the miR-124 and *IQGAP1* expression levels. Likewise, the expression of miR-124 negatively correlated with the *Vimentin* levels (Figure 4A, 4B, 4D). We also observed a positive correlation between miR-124 and *E-cadherin* expression in the EC tissues (Figure 4A, 4C). To investigate whether the down-regulation of miR-124 is associated with clinical outcomes in EC, we analyze data from 309 EC patients in the Cancer Genome Atlas (TCGA) database by using the SurvMicro web tool [20]. In brief, SurvMicro uses the Cox model and the miRNA levels to give each sample a risk score, and EC patients were stratified into the high-risk (with a low probability of survival; above median of risk score; n = 154) or

low-risk (with a high probability of survival; below the median of risk score; n = 155) group. Kaplan–Meier survival analysis revealed that the overall survival rate in the high-risk group were marginally significantly lower than those in the low-risk group (P = 0.0694) and high-risk patients had lower miR-124 expression levels than the low-risk patients (Figure 4E, 4F). Collectively, these data suggest that miR-124 expression is inversely correlated with the IQGAP1 expression level, and decreased miR-124 expression may be associated with poor outcomes for patients with EC. This supports a model that the loss of miR-124 activates IQGAP1 and contributes to EMT and cancer cell invasiveness.

MiR-124 is epigenetically silenced in EC cells

To examine whether DNA methylation and histone modification could account for the downregulation of miR-124 in EC, we treated EC cells with 5-aza-2'-deoxycytidine (5-AZA; a DNA methylation inhibitor) and/or Trichostatin A (TSA; a histone deacetylase inhibitor). As expected, the tumor suppressor miR-34b was silenced by DNA methylation in the EC cells [16], as shown by its upregulation in the HI and HEC-1 cells treated with 5-AZA. The expression of miR-124 was significantly
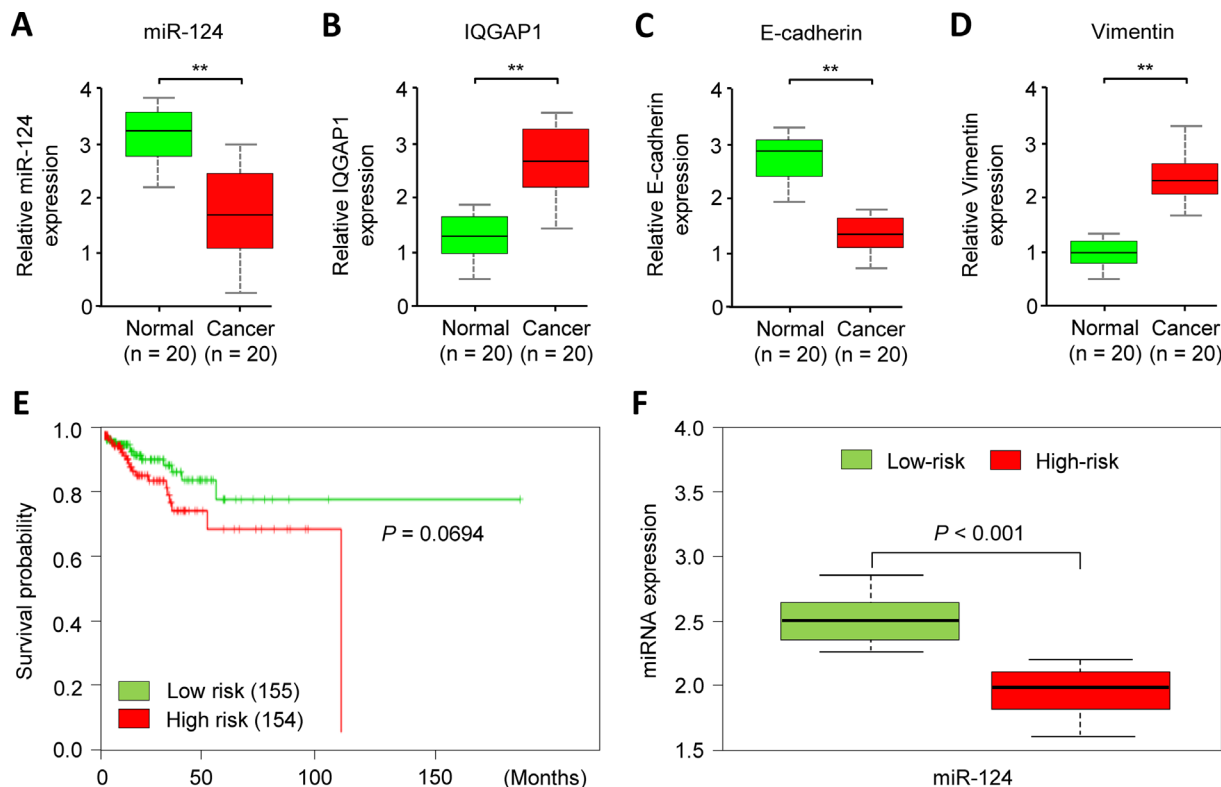

Figure 4: MiR-124 down-regulation is associated with elevated IQGAP1 expression in endometrial cancer cells. A-D. The expression levels of miR-124 (A), *IQGAP1* (B), *E-cadherin* (C), and *Vimentin* (D) were assessed by a quantitative PCR analysis of 20 paired cancerous and normal tissue samples from endometrial cancer patients. **E.** A Kaplan-Meier survival curve of 309 TCGA (Cancer Genome Atlas database) endometrial cancer samples was created using the SurvMicro database based on the low or high risk for a poor outcome. **F.** Box plots demonstrating significantly lower levels of miR-124 expression in the high-risk patients.

increased after treating with 5-AZA or a combination of 5-AZA plus TSA (Figure 5A, 5B), but the miR-124 and miR-34b levels remained relatively unchanged in cells treated with TSA alone (Figure 5A, 5B). Treatment with 5-AZA consistently down-regulated the IQGAP1 protein levels (Figure 5C) and markedly reduced cell proliferation and invasion (Figure 5D). These studies suggest that methylation-mediated silencing rather than histone modification serves as an epigenetic event that negatively regulates miR-124 expression. This repression of miR-124 in the EC cells results in the increased abundance of the key oncoprotein IQGAP1 and the subsequent induction of EMT.

DISCUSSION

IQGAP1 is often overexpressed in many solid tumors (other than EC) and is a key promoter of the EMT program, tumor cell migration, invasion, proliferation and angiogenesis [6-13, 21, 22]. Here we have shown that IQGAP1 induces EMT and enhances EC invasion, and also identified miR-124 as an epigenetically silenced tumor suppressor that inhibits the EC cell migration, invasion and proliferation, by down-regulating oncogene IQGAP1 expression.

The scaffolding protein IQGAP1 functions as a molecular hub for integrating and mediating multiple signaling pathways to promote both tumorigenesis and metastasis [23]. IQGAP1 can affect a wide range of cellular functions by interacting with kinases and other signaling molecules such as Cdc42 [24], Rac1 [25],

β-catenin [25], B-Raf [26], extracellular signal-regulated kinase (ERK) [27] and E-cadherin [11]. We show here that IQGAP1 expression is significantly increased in EC tissues. According to our gain- and loss-of-function experiments, IQGAP1 promoted proliferation and induced EMT, which facilitates the migration and invasion of EC cells. Our results provide the first *in vitro* evidence for oncogenic functions of IQGAP1 in EC cells, implying that it could potentially serve as a potential biomarker for the diagnosis and treatment of EC. Interestingly, the disruption of IQGAP1-ERK1/2 interactions with a specific IQGAP1 peptide has been shown to inhibit RAS- and RAF-driven tumorigenesis [28]. Therefore, inhibiting IQGAP1 functions may be a promising targeted therapy for tumors.

Our microarray analysis demonstrated an interesting mRNA expression profile and revealed 29 miRNAs that are significantly down-regulated in highly invasive cells relative to their parental lines. Among these miRNAs, let-7 family members such as let-7f [29], miR-34a [30], miR-127 [31], miR-148a [32], miR-424 [33] and miR-497 [34] are known to display tumor suppressor effects in tumors. In EC, miR-30a-5p expression levels are decreased [35] and the reduced expression of miR-29b correlates with poor disease-free survival [36]. The biological functions and mechanisms of these miRNAs in EC warrant further studies.

MiR-124 exerts tumor suppressor effects and is frequently methylated in multiple cancer types [17]. We demonstrated that miR-124 is down-regulated in EC and the loss of its expression is at least partly mediated by

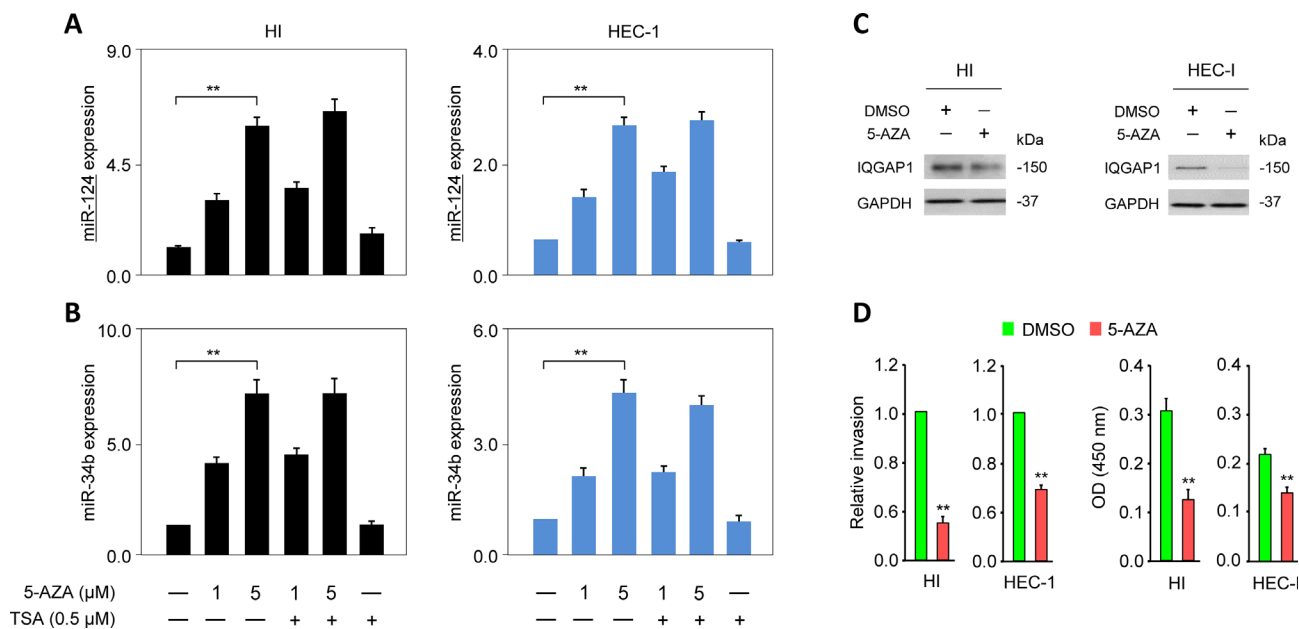**Figure 5: MiR-124 is epigenetically silenced in endometrial cancer cells. A, B.** HI and HEC-1 cells were treated with 5-aza-2'-deoxycytidine (5-AZA), Trichostatin A, or both, after which, quantitative PCR was used to measure the expression levels of miR-124 (A) and miR-34b (B). **C, D.** IQGAP1 protein levels (C), invasion, and proliferation (D) in endometrial cancer cells after treating with 5-AZA.

DNA methylation. Overexpressing miR-124 reverses EMT-like phenotypes and reduces EC cell migration, invasion and proliferation. Thus, the restoration of miR-124 by targeted delivery system or by treatment with DNA-demethylating agents may be therapeutically efficacious for the treatment of EC.

In conclusion, our findings provide a new mechanism that accounts for the observed downregulation of miR-124 and upregulation of IQGAP1 in EC. The methylation-mediated repression of miR-124 leads to the overexpression of IQGAP1, which in turn accelerates cancer cell proliferation, EMT and invasion.

MATERIALS AND METHODS

Patient samples

After informed consent, 20 pairs of primary ECs and adjacent non-tumor endometrial tissues [37] were collected according to an institutional Review Board-approved protocol at Cancer Center, Sun Yat-Sen University in China. Samples were snap-frozen and stored in liquid nitrogen until the RNA was extracted.

Cell culture and transfection

The human EC cell lines HEC-1 and HEC-50 were purchased from the JCRB Cell Bank (Osaka. Japan) and cultured in DMEM/F12 medium (Sigma-Aldrich, St. Louis, MO, USA) supplemented with 10% fetal bovine serum (FBS; Invitrogen, Carlsbad, CA, USA). Highly invasive HI cells were established as previously described [3]. The immortalized human endometrial epithelial cell line EM [38] was maintained in DMEM/F12 medium supplemented with 15% FBS. The human cervical cancer cell line, HeLa (ATCC, USA), was grown in DMEM/F12 medium supplemented with 10% FBS. The miR-124 mimic, negative control for the miRNA mimic, anti-miRNA inhibitor for miR-124, negative control for the miRNA inhibitor, IQGAP1 siRNA, and negative control siRNA were all purchased from Ambion (TX, USA). The miRNAs (30 nM) and siRNAs (5 nM) were transiently transfected into cells using Lipofectamine 2000 (Invitrogen, CA, USA) as described by the manufacturer. The pEGFR-IQGAP1-WT vector containing the IQGAP1 cDNA (IQGAP1 vector) and the pEGFR empty control vector, kindly provided by Professor Kozo Kaibuchi (Department of Cell Pharmacology, Nagoya University, Japan), were transiently transfected using the Lipofectamine Plus reagent (Invitrogen, CA, USA). The control vector and a human IQGAP1 cDNA vector lacking the 3'-UTR sequence were obtained from OriGene (MD, USA).

RNA isolation and qPCR

Total RNA for the microarray and qPCR analyses was extracted using TRIzol (Invitrogen, CA, USA) per the manufacturer protocol. The PrimeScript RT reagent kit (Takara, Japan) was used for the reverse transcription reaction with 100 ng of total RNA. The qPCR gene analysis was performed with Takara SYBR Premix Ex Taq II (Takara, Japan). Primers specific to *IQGAP1* [39] and *GAPDH* [40], which was used as an endogenous control for mRNA expression, have been previously described. Primers for *ZO-1*, *CK-18*, and *Vimentin* were obtained from the PrimerBank database (http://pga.mgh.harvard.edu/primerbank/). miRNA expression was detected by using the NCode miRNA qRT–PCR kit (Invitrogen, CA, USA) according to manufacturer's instructions. The forward primers used for the miRNA quantification were the same exact sequences of the mature miRNA genes. A universal reverse primer was provided in the NCode SYBR miRNA qRT-PCR kit. All miRNA quantification data were normalized to U6 small nuclear RNA [41] and *GAPDH* expression [42] and relative levels were calculated using the $2^{-\Delta\Delta Ct}$ method.

MiRNA microarray

The microarray analysis was performed using the Superprint G3 Human GE 8 × 60k Microarray (Agilent Technologies) as previously described [43]. The array covers all miRNA transcripts available in the latest version of the Sanger miRBase database. Briefly, total RNA was extracted from EC cells using TRIzol and was purified with the RNeasy MinElute Cleanup kit. MiRNA labeling, hybridization, and washing were performed as described by the manufacturer. Data pre-processing and the differential analysis of the miRNA expression data was done using the AgiMicroRna Bioconductor library. The expression level of miRNAs over 1.5 fold in HI cells with $P < 0.05$ was used as the cutoff to determine the significance compared to their parental HEC-50 cells.

Western blot

Total protein was collected 48 hours after transfection using the M-Per Mammalian Protein Extraction Reagent (Pierce Biotechnology, MA, USA) as described by the manufacturer. The proteins (40 μg) were separated by SDS-PAGE and transferred to polyvinylidene difluoride membranes for immunoblots with antibodies to IQGAP1 (2C5; Novus Biologicals), E-cadherin (A01589; GenScript), N-cadherin (#610920; BD), and GAPDH (sc-47724; Santa Cruz). These primary antibodies were used at a dilution of 1:1000.

Cell migration, invasion and proliferation assays

The transwell migration and invasion assay was performed as previously described [3, 4] with transfected cells seeded into the upper chamber (BD Biosciences, MA) with or without a Matrigel coating and DMEM/F12 with 10% FBS in the lower compartment acting as

a chemoattractant. Cells were allowed to migrate for 12 and 24 hours in the migration and invasion assays, respectively. The non-motile cells were removed from the top, and the cells in the bottom chamber were stained and counted under a light microscope. Relative migration and invasion activities are expressed as the fold-change over their respective controls. The effect of IQGAP1 or miR-124 on proliferation was measured using Cell Counting Kit-8 (Dojindo, Japan). Briefly, 5×10^3 cells were plated in 96-well plates for 24 hours and then transfected with the IQGAP1 cDNA vector/IQGAP1 siRNA, miR-124 mimics/inhibitors, and their respective controls. At 72 hours, the absorbance of the cells was measured with a spectrophotometer at 450 nm.

Luciferase activity assay

The Renilla luciferase-reporter plasmids containing human *IQGAP1* mRNA [44] with either wild-type (Wt; #14503) or mutant (Mut; #14504) miR-124 binding sites (875–882 bp and 1172–1178 bp from the start site of the 3'-UTR) were obtained from Addgene (Cambridge, MA, USA). Wt or Mut IQGAP1 reporter vectors, together with the pGL3-basic firefly luciferase expression vector as a reference control (Promega, San Luis Obispo, CA, USA), were transfected with 30 nM of the miR-124 mimic or inhibitor using Lipofectamine 2000 (Invitrogen, CA, USA). The Renilla and firefly luciferase activities were measured using the Dual Luciferase assay kit (Promega, WI, USA) 24 hours after transfection. The Renilla luciferase activity was normalized to the firefly luciferase activity.

Drug treatment

Cells were treated with 5-AZA (1 or 5 μM; Sigma-Aldrich) for 72 hours or TSA (0.5 μM; Sigma-Aldrich) for 24 hours. For the combination study, the 5-AZA (5 μM) was present for 72 hours and the TSA (0.5 μM) was added for the last 24 hours. The media were changed daily, and fresh drug was added.

Statistical analysis

Data are presented as the mean ± SEM of at least three independent experiments performed in triplicate. If not specified otherwise, the experimental values are expressed as fold-changes normalized to their respective controls. Statistical significance was assessed by the two-tailed Student t-test ($*P < 0.05$; $**P < 0.01$). The differences between the cancer and normal tissues were analyzed using the Wilcoxon matched-pairs test.

CONFLICTS INTERESTS

GRANT SUPPORT

REFERENCES

1. Mitra A, Mishra L, Li S. EMT, CTCs and CSCs in tumor relapse and drug-resistance. Oncotarget. 2015; 6:10697–10711. doi: 10.18632/oncotarget.4037.

2. Dong P, Kaneuchi M, Konno Y, Watari H, Sudo S, Sakuragi N. Emerging therapeutic biomarkers in endometrial cancer. Biomed Res Int. 2013; 2013:130362.

3. Dong P, Kaneuchi M, Watari H, Hamada J, Sudo S, Ju J, Sakuragi N. MicroRNA-194 inhibits epithelial to mesenchymal transition of endometrial cancer cells by targeting oncogene BMI-1. Mol Cancer. 2011; 10:99.

4. Dong P, Karaayvaz M, Jia N, Kaneuchi M, Hamada J, Watari H, Sudo S, Ju J, Sakuragi N. Mutant p53 gain-of-function induces epithelial-mesenchymal transition through modulation of the miR-130b-ZEB1 axis. Oncogene. 2013; 32:3286–3295.

5. Mateer SC, McDaniel AE, Nicolas V, Habermacher GM, Lin MJ, Cromer DA, King ME, Bloom GS. The mechanism for regulation of the F-actin binding activity of IQGAP1 by calcium/calmodulin. J Biol Chem. 2002; 277:12324–12333.

6. Noritake J, Watanabe T, Sato K, Wang S, Kaibuchi K. IQGAP1: a key regulator of adhesion and migration. J Cell Sci. 2005; 118:2085–2092.

7. Nabeshima K, Shimao Y, Inoue T, Koono M. Immunohistochemical analysis of IQGAP1 expression in human colorectal carcinomas: its overexpression in carcinomas and association with invasion fronts. Cancer Lett. 2002; 176:101–109.

8. Dong P, Nabeshima K, Nishimura N, Kawakami T, Hachisuga T, Kawarabayashi T, Iwasaki H. Overexpression and diffuse expression pattern of IQGAP1 at invasion fronts are independent prognostic parameters in ovarian carcinomas. Cancer Lett. 2006; 243:120–127.

9. Chen F, Zhu HH, Zhou LF, Wu SS, Wang J, Chen Z. IQGAP1 is overexpressed in hepatocellular carcinoma and promotes cell proliferation by Akt activation. Exp Mol Med. 2010; 42:477–483.

10. Wang XX, Li XZ, Zhai LQ, Liu ZR, Chen XJ, Pei Y. Overexpression of IQGAP1 in human pancreatic cancer. Hepatobiliary Pancreat Dis Int. 2013; 12:540–545.

11. Kuroda S, Fukata M, Nakagawa M, Fujii K, Nakamura T, Ookubo T, Izawa I, Nagase T, Nomura N, Tani H, Shoji I, Matsuura Y, Yonehara S, Kaibuchi K. Role of IQGAP1, a target of the small GTPases Cdc42 and Rac1, in regulation of E-cadherin- mediated cell-cell adhesion. Science. 1998; 281:832–835.

12. Liu Z, Liu D, Bojdani E, El-Naggar AK, Vasko V, Xing M. IQGAP1 plays an important role in the invasiveness of thyroid cancer. Clin Cancer Res. 2010; 16:6009–6018.

13. Wang XX, Wang K, Li XZ, Zhai LQ, Qu CX, Zhao Y, Liu ZR, Wang HZ, An QJ, Jing LW, Wang XH. Targeted knockdown of IQGAP1 inhibits the progression of esophageal squamous cell carcinoma *in vitro* and *in vivo*. PLoS One. 2014; 9:e96501.

14. Yan J, Gumireddy K, Li A, Huang Q. Regulation of mesenchymal phenotype by MicroRNAs in cancer. Curr Cancer Drug Targets. 2013; 13:930–934.

15. Kiesslich T, Pichler M, Neureiter D. Epigenetic control of epithelial-mesenchymal-transition in human cancer. Mol Clin Oncol. 2013; 1:3–11.

16. Hiroki E, Suzuki F, Akahira J, Nagase S, Ito K, Sugawara J, Miki Y, Suzuki T, Sasano H, Yaegashi N. MicroRNA-34b functions as a potential tumor suppressor in endometrial serous adenocarcinoma. Int J Cancer. 2012; 131:E395–404.

17. Suzuki H, Maruyama R, Yamamoto E, Kai M. DNA methylation and microRNA dysregulation in cancer. Mol Oncol. 2012; 6:567–578.

18. Furuta M, Kozaki KI, Tanaka S, Arii S, Imoto I, Inazawa J. miR-124 and miR-203 are epigenetically silenced tumor-suppressive microRNAs in hepatocellular carcinoma. Carcinogenesis. 2010; 31:766–776.

19. Sun G, Liu Y, Wang K, Xu Z. miR-506 regulates breast cancer cell metastasis by targeting IQGAP1. Int J Oncol. 2015; 47:1963–1970.

20. Aguirre-Gamboa R, Trevino V. SurvMicro: assessment of miRNA-based prognostic signatures for cancer clinical outcomes by multivariate survival analysis. Bioinformatics. 2014; 30:1630–1632.

21. Moon H, Ruelcke JE, Choi E, Sharpe LJ, Nassar ZD, Bielefeldt-Ohmann H, Parat MO, Shah A, Francois M, Inder KL, Brown AJ, Russell PJ, Parton RG, Hill MM. Diet-induced hypercholesterolemia promotes androgen-independent prostate cancer metastasis via IQGAP1 and caveolin-1. Oncotarget. 2015; 6:7438–7453. doi: 10.18632/oncotarget.3476.

22. Dong PX, Jia N, Xu ZJ, Liu YT, Li DJ, Feng YJ. Silencing of IQGAP1 by shRNA inhibits the invasion of ovarian carcinoma HO-8910PM cells *in vitro*. J Exp Clin Cancer Res. 2008; 27:77.

23. Smith JM, Hedman AC, Sacks DB. IQGAPs choreograph cellular signaling from the membrane to the nucleus. Trends Cell Biol. 2015; 25:171–184.

24. Hart MJ, Callow MG, Souza B, Polakis P. IQGAP1, a calmodulin- binding protein with a RasGAP-related domain, is a potential effector for Cdc42Hs. EMBO J. 1996; 15:2997–3005.

25. Fukata M, Kuroda S, Nakagawa M, Kawajiri A, Itoh N, Shoji I, Matsuura Y, Yonehara S, Fujisawa H, Kikuchi A, Kaibuchi K. Cdc42 and Rac1 regulate the interaction of IQGAP1 with β-catenin. J Biol Chem. 1999; 274:26044–26050.

26. Ren JG, Li Z, Sacks DB. IQGAP1 modulates activation of B-Raf. Proc Natl Acad Sci U S A. 2007; 104:10465–10469.

27. Roy M, Li Z, Sacks DB. IQGAP1 is a scaffold for mitogen-activated protein kinase signaling. Mol Cell Biol. 2005; 25:7940–7952.

28. Jameson KL, Mazur PK, Zehnder AM, Zhang J, Zarnegar B, Sage J, Khavari PA. IQGAP1 scaffold-kinase interaction blockade selectively targets RAS-MAP kinase–driven tumors. Nat Med. 2013; 19:626–630.

29. Liang S, He L, Zhao X, Miao Y, Gu Y, Guo C, Xue Z, Dou W, Hu F, Wu K, Nie Y, Fan D. MicroRNA let-7f inhibits tumor invasion and metastasis by targeting MYH9 in human gastric cancer. PLoS One. 2011; 6:e18409.

30. Li XJ, Ren ZJ, Tang JH. MicroRNA-34a: a potential therapeutic target in human cancer. Cell Death Dis. 2014; 5:e1327.

31. Lujambio A, Esteller M. CpG island hypermethylation of tumor suppressor microRNAs in human cancer. Cell Cycle. 2007; 6:1455–1459.

32. Sakamoto N, Naito Y, Oue N, Sentani K, Uraoka N, Zarni Oo H, Yanagihara K, Aoyagi K, Sasaki H, Yasui W. MicroRNA-148a is downregulated in gastric cancer, targets MMP7, and indicates tumor invasiveness and poor prognosis. Cancer Sci. 2014; 105:236–243.

33. Li Q, Qiu XM, Li QH, Wang XY, Li L, Xu M, Dong M, Xiao YB. MicroRNA-424 may function as a tumor suppressor in endometrial carcinoma cells by targeting E2F7. Oncol Rep. 2015; 33:2354–2360.

34. Yan JJ, Zhang YN, Liao JZ, Ke KP, Chang Y, Li PY, Wang M, Lin JS, He XX. MiR-497 suppresses angiogenesis and metastasis of hepatocellular carcinoma by inhibiting VEGFA and AEG-1. Oncotarget. 2015; 6:29527–29542. doi: 10.18632/oncotarget.5012.

35. Tsukamoto O, Miura K, Mishima H, Abe S, Kaneuchi M, Higashijima A, Miura S, Kinoshita A, Yoshiura K, Masuzaki H. Identification of endometrioid endometrial carcinoma-associated microRNAs in tissue and plasma. Gynecol Oncol. 2014; 132:715–721.

36. Hiroki E, Akahira J, Suzuki F, Nagase S, Ito K, Suzuki T, Sasano H, Yaegashi N. Changes in microRNA expression levels correlate with clinicopathological features and prognoses in endometrial serous adenocarcinomas. Cancer Sci. 2010; 101:241–249.

37. Dong P, Kaneuchi M, Xiong Y, Cao L, Cai M, Liu X, Guo SW, Ju J, Jia N, Konno Y, Watari H, Hosaka M, Sudo S, Sakuragi N. Identification of KLF17 as a novel

epithelial to mesenchymal transition inducer via direct activation of TWIST1 in endometrioid endometrial cancer. Carcinogenesis. 2014; 35:760–768.

38. Kyo S, Nakamura M, Kiyono T, Maida Y, Kanaya T, Tanaka M, Yatabe N, Inoue M. Successful immortalization of endometrial glandular cells with normal structural and functional characteristics. Am J Pathol. 2003; 163:2259–2269.

39. Roy M, Li Z, Sacks DB. IQGAP1 Binds ERK2 and Modulates Its Activity. J Biol Chem. 2004; 279:17329–17337.

40. Figueira RC, Gomes LR, Neto JS, Silva FC, Silva ID, Sogayar MC. Correlation between MMPs and their inhibitors in breast cancer tumor tissue specimens and in cell lines with different metastatic potential. BMC Cancer. 2009; 9:20.

41. Prasad R, Katiyar SK. Down-regulation of miRNA-106b inhibits growth of melanoma cells by promoting G1-phase cell cycle arrest and reactivation of p21/WAF1/Cip1 protein. Oncotarget. 2014; 5:10636–10649. doi: 10.18632/oncotarget.2527.

42. Chen R, Alvero AB, Silasi DA, Kelly MG, Fest S, Visintin I, Leiser A, Schwartz PE, Rutherford T, Mor G. Regulation of IKKbeta by miR-199a affects NF-kappaB activity in ovarian cancer cells. Oncogene. 2008; 27:4712–4723.

43. Konno Y, Dong P, Xiong Y, Suzuki F, Lu J, Cai M, Watari H, Mitamura T, Hosaka M, Hanley SJ, Kudo M, Sakuragi N. MicroRNA-101 targets EZH2, MCL-1 and FOS to suppress proliferation, invasion and stem cell-like phenotype of aggressive endometrial cancer cells. Oncotarget. 2014; 5: 6049–6062. doi:10.18632/oncotarget.2157.

44. Lim LP, Lau NC, Garrett-Engele P, Grimson A, Schelter JM, Castle J, Bartel DP, Linsley PS, Johnson JM. Microarray analysis shows that some microRNAs downregulate large numbers of target mRNAs. Nature. 2005; 433:769–773.

Case Report

A Case of Thanatophoric Dysplasia Type I with Fetal Hydrops in the First Trimester

Giannina Calongos,[1] Masateru Hori,[1] Mai Ogino,[1] and Hideaki Sawai[2]

[1]*Department of Obstetrics and Gynecology, Meiwa General Hospital, Nishinomiya 663-8186, Japan*
[2]*Department of Obstetrics and Gynecology, Hyogo College of Medicine, Nishinomiya 663-8501, Japan*

Correspondence should be addressed to Giannina Calongos; calongos.g@meiwa-hospital.com

During a routine prenatal exam, a 36-year-old female in her third pregnancy was diagnosed with fetal hydrops at 11 weeks of gestation. The pregnancy was monitored with periodic ultrasounds; however, spontaneous resolution was not observed. Amniotic fluid examination at 16 weeks of gestation showed a normal karyotype; however, macrocephaly, a narrow thorax, and shortening of the long bones were observed on ultrasonography. With the strong suspicion of a fetal skeletal disease, specifically thanatophoric dysplasia (TD), and after extensive genetic counseling, termination of the pregnancy was performed per the parents' wishes with mechanical cervical dilation and gemeprost (PGE1) administration. Following delivery, the fetus was found to have macrocephaly, a narrow bell-shaped thorax, and a protuberant abdomen, as well as curved long bones, H-shaped platyspondyly, and curved clavicles on skeletal radiography. As a result, the fetus was diagnosed with TD type I. This case illustrates that although TD is a rare disease, an accurate prenatal diagnosis can be made with the use of ultrasonography.

1. Introduction

Thanatophoric dysplasia (TD) is a rare and lethal skeletal dysplasia with an estimated incidence of 1 in 20000 to 40000 births [1] and was first described by Maroteaux et al. in 1967 [2]. TD can be classified into two types: type I is characterized by micromelia with bowed femurs and, uncommonly, the presence of cloverleaf skull deformity; type II is characterized by micromelia with straight femurs and moderate to severe cloverleaf skull deformity [3]. A common feature to both types is the presence of a narrow thorax which causes respiratory failure shortly after birth [4, 5].

Fetal hydrops is defined as an abnormal fluid collection in two or more areas of the fetal body. It can be further classified as immune or nonimmune. Immune fetal hydrops develops due to fetal hemolysis secondary to incompatibility of maternal and fetal blood type. Nonimmune hydrops, on the other hand, can result from a large number of causes [6, 7]. However, 20–30% of hydrops is of unknown etiology.

Here, we report a case of TD type I with fetal hydrops diagnosed in the first trimester and thereafter shortening of the long bones and macrocephaly. Confirmation of the diagnosis was made by clinical examination and radiologic studies after delivery.

2. Case Presentation

A 36-year-old female in her third pregnancy came to our hospital at 8 weeks of gestation for a routine prenatal check. The couple and their previous children's past and family histories were unremarkable. Ultrasonographic examination at 8 weeks of gestation was unremarkable, with a crown-rump length (CRL) of 15.9 mm. At 11 weeks of gestation, although the CRL was 49.6 mm corresponding to gestational age, fetal hydrops was evident on ultrasonography (Figure 1(a)). Since screening for immune hydrops and congenital infections were negative, a transvaginal ultrasound was performed the following week for further evaluation. At 12 weeks of gestation, appropriate fetal growth was observed with a CRL of 60 mm; however, fetal hydrops was still present. The couple was counseled on the different etiologies of fetal hydrops; however, at this point the cause was not clear.
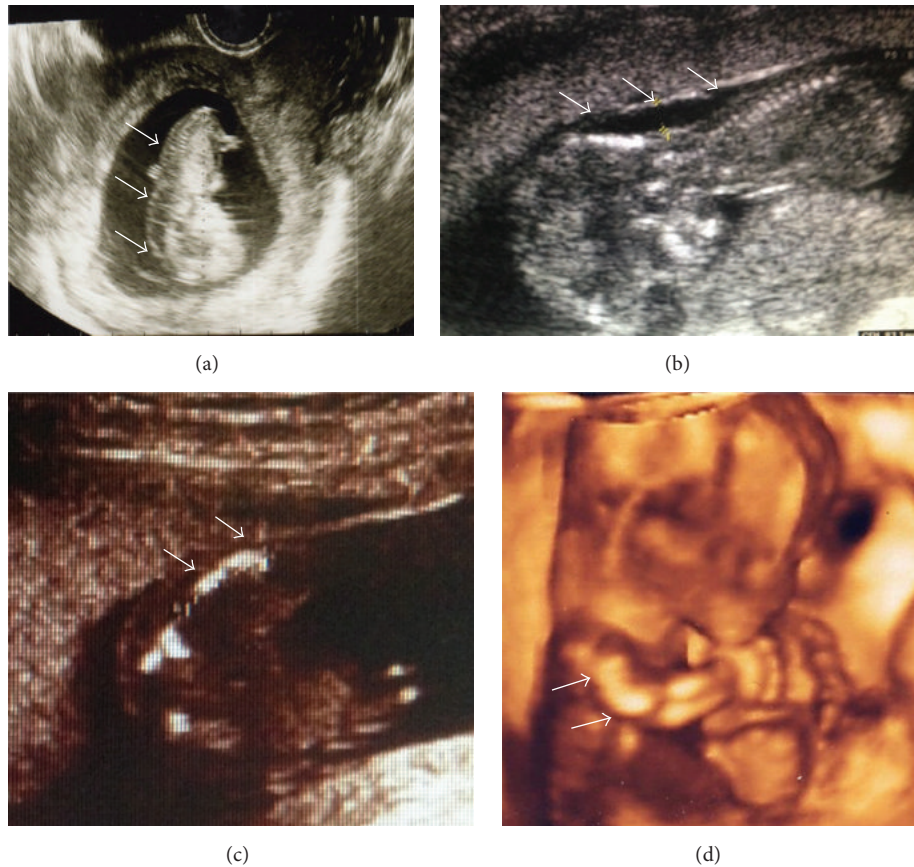
(a)

(b)

(c)

(d)

FIGURE 1: Fetal ultrasound with skin edema in the posterior part of the head and vertebral column (→) (a). A longitudinal view of the head and the thorax demonstrating skin edema in the posterior part of the neck (→), macrocephaly, and narrow thorax (b). Fetal ultrasound showing short curved femur (→) (c). A three-dimensional image with a view of the upper limbs showing bowed humerus (→) (d).

At 13 weeks of gestation the biparietal diameter (BPD) was measured to be 27.4 mm, corresponding to the 95th percentile. From this week on macrocephaly was observed and a narrow thorax was suspected on subsequent ultrasonographies (Figure 1(b)). At 16 weeks of gestation, amniotic fluid examination showed a normal karyotype (46XX); however, a routine and a four-dimensional ultrasound revealed shortening and bowing of the long bones (femur length (FL) 11.6 mm) (Figures 1(c) and 1(d)) with no subsequent improvement. As a result, a fetal skeletal disease, specifically TD, was strongly suspected. At 20 weeks of gestation, the FL was 1.18 cm, compatible with less than the 5th percentile. Also, the BPD was 5.3 cm, corresponding to more than the 95th percentile. During genetic counseling, a molecular analysis was suggested to the parents in order to make an accurate prenatal diagnosis of TD; however, they opted not to pursue this exam and decided on termination of the pregnancy, instead. The patient was then hospitalized and underwent mechanical cervical dilation. The following day gemeprost (PGE1) was administered intravaginally every three hours. A 400 g female fetus was delivered dead at 20 weeks and 2 days of gestation (Figure 2). All limbs were noted to be extremely short with redundant skin folds. Macrocephaly was evident. A narrow bell-shaped thorax with short ribs

and a protuberant abdomen were noticed; however, the skull and facial characteristics were within normal limits. Skeletal radiography showed telephone receiver-like curved femurs and humeri accompanied by irregular metaphyses, an H-shaped platyspondyly, and curved clavicles (Figure 3). No cloverleaf skull deformity was observed. These characteristics confirmed the diagnosis of TD type I.

3. Discussion

The incidence of immune hydrops has decreased due to routine screening and prophylaxis; however, the mortality rate of nonimmune hydrops, during either the fetal or the neonatal period, is up to 75.5% [8]. Although fetal hydrops is considered to be a nonspecific finding on obstetric ultrasounds, previous reports showed that an increased nuchal translucency (NT) and hydrops are common features of serious skeletal dysplasia [9]. Moreover, previous cases of TD reported a NT of 3.4–6.5 mm by 14 weeks of gestation which correlates with the 5.7 mm observed in this case [9].

As previous studies reported, 40–80% of TD cases can be correctly diagnosed by ultrasonography in the prenatal period [10]. Limb shortening in TD is also sonographically apparent from as early as 13 weeks of gestation. Similarly,

FIGURE 2: Female fetus of 20 weeks of pregnancy with short limbs and redundant skin folds. Also, macrocephaly, narrow bell-shaped thorax, and protuberant abdomen were noticed. Skull and facial characteristics were normal.
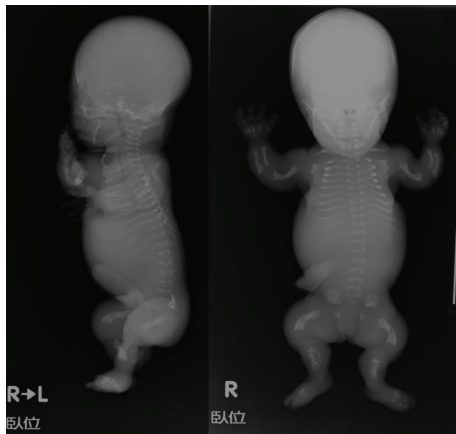

FIGURE 3: Anteroposterior and lateral radiographs of the fetus showing telephone receiver-like curved femurs and humeri with irregular metaphyses, H-shaped platyspondyly, and curved clavicles. No cloverleaf skull deformity was observed.

head circumference (HC) is increased throughout gestation, a feature that is present as early as the first trimester [10]. With the evidence of short limbs, a hypoplastic thorax, and macrocephaly, we strongly suspected a skeletal disease as TD.

Published reports have used a femur length/abdominal circumference (FL/AC) ratio <0.16 as a predictor for lethal skeletal dysplasia [11]. Also, a hypoplastic thorax is suspected with a thoracic circumference of less than 5% at the level of the four-chamber view of the heart or a thoracic-AC ratio of less than 0.79 [12]. In this case the FL/AC ratio was 0.103 (0.82 cm/7.9 cm) and 0.0769 (1.18 cm/15.34 cm) at 13 and 20 weeks of pregnancy, respectively. A narrow bell-shaped thorax was suspected as early as 13 weeks of pregnancy.

TD is the most frequent lethal skeletal dysplasia caused by mutation of the fibroblast growth factor 3 (FGFR3) gene [13, 14]. Although molecular analysis of fetal cells to detect Arg248Cys, Tyr373Cys, Lys650Glu, and other specific mutations enables an accurate prenatal diagnosis of TD [1], it was not performed in this case per the couple's wishes. However, since limb shortening is associated with a 2.7 relative risk for trisomy 21 [4] and a case of TD type I presented with trisomy 21 was reported previously [15], we considered an amniocentesis at 16 weeks of gestation important to perform. TD is an autosomal dominant genetic disease; however, it is almost always caused by a de novo mutation in FGFR3 [3]. As a result, a general empiric recurrence risk is estimated in only 2% [16]. This fact is important to consider in order to relieve parental anxiety over future pregnancies. After counseling, the patient had a fourth pregnancy without complications and delivered a normal female baby at term.

In summary, even though TD is a rare condition, ultrasonography can be used to obtain an accurate prenatal diagnosis and facilitate early parental counseling.

Conflict of Interests

The authors declare that there is no conflict of interests regarding the publication of this paper.

References

[1] H. Sawai, S. Komori, A. Ida, T. Henmi, T. Bessho, and K. Koyama, "Prenatal diagnosis of thanatophoric dysplasia by mutational analysis of the fibroblast growth factor receptor 3 gene and a proposed correction of previously published PCR results," *Prenatal Diagnosis*, vol. 19, no. 1, pp. 21–24, 1999.

[2] P. Maroteaux, M. Lamy, and J. M. Robbert, "Le nanisme thanatophore," *La Presse Médicale*, vol. 49, pp. 2519–2524, 1967.

[3] B. Karczeski and G. R. Cutting, "Thanatophoric dysplasia," in *GeneReviews*, NCBI Bookshelf, 2013.

[4] G. Nishimura, J. Murotsuki, and H. Sawai, "Fetal diagnosis and perinatal management of skeletal dysplasias. Medical View," *Sawai H. Fetal diagnosis and perinatal management of skeletal dysplasias. Medical View*, p. 122, 2011.

[5] S. M. Nikkel, N. Major, and W. J. King, "Growth and development in thanatophoric dysplasia—an update 25 years later," *Clinical Case Reports*, vol. 1, no. 2, pp. 75–78, 2013.

[6] K. Amano and Y. Ushibashi, *Compact Atlas of Obstetrics and Gynecology Ultrasound*, Vector Core, 2012.

[7] W. Yeom, E. S. Paik, J.-J. An et al., "Clinical characteristics and perinatal outcome of fetal hydrops," *Obstetrics & Gynecology Science*, vol. 58, no. 2, pp. 90–97, 2015.

[8] M. E. Abrams, K. S. Meredith, P. Kinnard, and R. H. Clark, "Hydrops fetalis: a retrospective review of cases reported to a large national database and identification of risk factors associated with death," *Pediatrics*, vol. 120, no. 1, pp. 84–89, 2007.

[9] A. Khalil, E. Pajkrt, and L. S. Chitty, "Early prenatal diagnosis of skeletal anomalies," *Prenatal Diagnosis*, vol. 31, no. 1, pp. 115–124, 2011.

[10] L. S. Chitty, A. Khalil, A. N. Barrett, E. Pajkrt, D. R. Griffin, and T. J. Cole, "Safe, accurate, prenatal diagnosis of thanatophoric dysplasia using ultrasound and free fetal DNA," *Prenatal Diagnosis*, vol. 33, no. 5, pp. 416–423, 2013.

[11] A. Rahemtullah, B. McGillivray, and R. D. Wilson, "Suspected skeletal dysplasias: femur length to abdominal circumference ratio can be used in ultrasonographic prediction of fetal outcome," *American Journal of Obstetrics and Gynecology*, vol. 177, no. 4, pp. 864–869, 1997.

[12] A. Johnson, N. A. Callan, and V. K. Bhutani, "Ultrasonic ratio of fetal thoracic to abdominal circumference: an association with fetal pulmonary hypoplasia," *American Journal of Obstetrics & Gynecology*, vol. 157, no. 3, pp. 764–769, 1987.

[13] P. L. Tavormina, R. Shiang, L. M. Thompson et al., "Thanatophoric dysplasia (types I and II) caused by distinct mutations in fibroblast growth factor receptor 3," *Nature Genetics*, vol. 9, no. 3, pp. 321–328, 1995.

[14] L. Legeai-Mallet, C. Benoist-Lasselin, A.-L. Delezoide, A. Munnich, and J. Bonaventure, "Fibroblast growth factor receptor 3 mutations promote apoptosis but do not alter chondrocyte proliferation in thanatophoric dysplasia," *The Journal of Biological Chemistry*, vol. 273, no. 21, pp. 13007–13014, 1998.

[15] T. Yamada, H. Sawai, G. Nishimura, H. Numabe, K. Cho, and H. Minakami, "Platyspondylic lethal skeletal dysplasia San Diego type (thanatophoric dysplasia type 1) associated with trisomy 21 presenting with nuchal translucency: a case report," *Prenatal Diagnosis*, vol. 29, no. 7, pp. 715–717, 2009.

[16] N. S. Naveen, B. V. Murlimanju, V. Kumar, T. Pulakunta, and H. Jeeyar, "Thanatophoric dysplasia: a rare entity," *Oman Medical Journal*, vol. 26, no. 3, pp. 196–197, 2011.

Follow-Up Study on Fetal CT Radiation Dose in Japan: Validating the Decrease in Radiation Dose

Osamu Miyazaki[1]
Hideaki Sawai[2]
Takahiro Yamada[3]
Jun Murotsuki[4,5]
Gen Nishimura[6]

[1]Department of Radiology, National Center for Child Health and Development, 2-10-1 Okura, Setagaya-ku, Tokyo 157-8535, Japan. Address correspondence to O. Miyazaki (miyazaki-o@ncchd.go.jp).

[2]Department of Obstetrics and Gynecology, Hyogo College of Medicine, Hyogo, Japan.

[3]Department of Obstetrics and Gynecology, Hokkaido University Graduate School of Medicine, Sapporo, Japan.

[4]Department of Maternal and Fetal Medicine, Miyagi Children's Hospital, Miyagi, Japan.

[5]Department of Advanced Fetal and Developmental Medicine, Tohoku University Graduate School of Medicine, Miyagi, Japan.

[6]Department of Pediatric Imaging, Tokyo Metropolitan Children's Medical Center, Tokyo, Japan.

OBJECTIVE. In 2011, we collected data on fetal CT radiation dose to determine the diagnostic reference level (DRL); however, continuous evaluation of the DRL is necessary. The hypothesis of this study is that the fetal CT radiation dose has decreased, and we predict a widespread use of iterative reconstruction (IR). We also predict that the national decrease in exposure is because of the DRL reported as a result of the previous national study.

MATERIALS AND METHODS. Various testing protocols from each site were summarized as part of the study results. The minimum, one-fourth (25th percentile), median, three-fourths (75th percentile), and maximum values were obtained for volume CT dose index (CTDI$_{vol}$), dose-length product (DLP), and scan length of 120 fetal CT examinations. The trends for IR usage and tube voltage were also investigated.

RESULTS. Compared to the results of the 2011 study ($n = 119$), the minimum, 25th percentile, median, and 75th percentile values for CTDI$_{vol}$ and DLP have decreased for the tabulated results in 2015 ($n = 120$). The 75th percentile value for CTDI$_{vol}$ was 4.9 mGy, which is 43% of the previous value. IR was used in 70% of the sites. The radiation dose was significantly lower among groups that used IR.

CONCLUSION. Four years passed between our initial survey on DRL and the present follow-up survey, and it appears that the previous report sufficiently fulfilled its objective and role in contributing to the decrease in DRL observed in this follow-up study.

According to an international classification issued in 2015 [1], there are 436 disease names, classified into 42 disease groups, and 364 responsible genes associated with genetic disease skeletal dysplasia. During the neonatal period, these diseases are found at a rate of two in 10,000 births, and half are lethal [2]. The recent widespread use of fetal ultrasound testing and improvement in diagnostic accuracy has led to the detection of short limbs and more cases of suspected skeletal dysplasia [3]. The advantage of ultrasound is that it can be used for pregnant women without involving x-ray irradiation. However, it is extremely difficult to detect, evaluate, and interpret the abnormal findings of skeletal structures using ultrasound, and a specific diagnosis cannot be made by the ultrasound operator without vast knowledge and experience in making such diagnoses. Unless the region that may contain the abnormalities is searched in detail during the scan, sufficient material for retrospective diagnosis cannot be obtained. This is the disadvantage of ultrasound testing that is based on real-time diagnosis.

However, the effectiveness of prenatal 3D CT for detecting fetal skeletal dysplasia has been previously reported, and 93% of pathognomonic abnormal findings confirmed after birth with simple x-ray were diagnosable with fetal skeletal CT. It was reported that the diagnosis determined by ultrasound was revised for about 60% of the cases after fetal CT [4].

Prenatal diagnosis using CT provides visual and clinical information to facilitate planning for a birthing method and selection of treatment by the various people involved, including the parents, family members, obstetrician, and perinatal care staff. It also allows the parents of the fetus to prepare themselves psychologically. Although there are many advantages, the risk of radiation exposure to the fetus and mother cannot be avoided because CT uses x-rays.

In 2011, we surveyed medical institutions in Japan that conduct fetal CT and collected data on CT conditions and radiation exposure; that study was published in 2014 [5].

From the data, we reported the estimated diagnostic reference level (DRL). To our knowledge, that report was the first and only fetal CT DRL study in the world. We decided to investigate DRL again in 2015 because 3 years and 9 months had passed since the initial survey was conducted. Periodic assessment of DRL every few years at each medical institution or at the national level is recommended [6]. Since the first study was conducted, CT equipment has seen further progress in the number of detectors, and high-performance CT equipment with 64 or more detectors are almost in common use. In addition, there are some reports in the pediatric radiology field that show an increase in popularity for using an iterative reconstruction (IR) protocol to reduce the radiation dose [7].

The hypothesis of this study is that the fetal CT radiation dose has decreased throughout the country compared with the nationwide study conducted in Japan in 2011 [5], and we predict the widespread usage of fetal CT with IR. We also predict that the national decrease in exposure is because of the DRL reported as a result of the previous national study.

Materials and Methods
Selection of Target Medical Institutions

This study was approved by the ethics board of the National Center for Child Health and Development and was conducted after approval of the institutional review board.

The 16 sites that were studied in the 2011 survey [5] are major facilities performing fetal CT in Japan and were included in this study. In addition, an Internet forum for fetal skeletal dysplasia based in Japan, the Japan Forum of Fetal Skeletal Dysplasia (with 53 registered users), was used to call for participation by medical institutions that did not participate in the previous study. Medical institutions that consulted the radiologist and obstetrician members of the forum were also selected as candidates. Furthermore, medical institutions that have presented results in past society meetings in Japan and overseas, or submitted journal papers, were sought and considered as candidates. As a result, 25 medical institutions were selected as study sites. These study sites were mailed a CD-ROM with the questionnaire sheet, together with a letter inquiring about their interest regarding participation. The following 22 medical institutions expressed interest: Hokkaido University Hospital; Aomori Prefectural Central Hospital; Miyagi Children's Hospital; Tohoku University Hospital; Yamaga-

ta University Hospital; Chiba Kaihin Municipal Hospital; Juntendo University Urayasu Hospital; National Center for Child Health and Development; Jikei University School of Medicine Hospital; Tokyo Women's Medical University Hospital; Fujita Health University Hospital; Nagara Medical Center; University Hospital, Kyoto Prefectural University of Medicine; Osaka Medical Center and Research Institute for Maternal and Child Health; Hyogo College of Medicine Hospital; Shikoku Medical Center for Children and Adults; Perinatal Medical Center, Ehime Prefectural Central Hospital; Kochi Health Sciences Center; Tokushima University Hospital; Hiroshima University Hospital; Perinatal Medical Center, Yamaguchi Prefectural Grand Medical Center; and Kurume University Hospital.

Preparation of the Work Sheet

The first page of the work sheet was to be entered by the obstetrician of the hospital, and the remaining pages were to be entered by the radiologic technologist or radiologist. Eight questions were listed on the first page. First, what is the category of your hospital (choice of three options: university hospital, perinatal medical center, or regional core hospital)? Second, was specific written consent for fetal CT obtained? Third, how many fetal CT examinations have been conducted in the past 3 years and 9 months? Fourth, at what range of fetal stage (weeks) was CT conducted and what was the mean number of weeks? Fifth, on the basis of the 2011 study [5], have there been any changes to the protocol? Sixth, if the protocol has been changed, has the diagnostic ability decreased as a result of lowering the dose? Seventh, is sedation used on the fetus when conducting fetal CT? Finally, do you know the approximate fetal CT radiation dose for your hospital?

The CT survey from the second page onward had entry sheets for four manufacturers: Toshiba, GE Healthcare, Siemens Healthcare, and Philips Healthcare. The sheet for the manufacturer of the equipment used for testing at each site was also filled out. If multiple pieces of CT equipment were used at one site, we requested that each piece was entered into separate work sheets. Because parameters are different depending on the manufacturer, the work sheet entry items tailored for each CT manufacturer were chosen by a subgroup of seven radiologic technologists selected from sites that frequently perform fetal CT. The staff in charge of setting imaging protocols for each manufacturer at each of the four CT manufacturers was requested to check for the appropriateness of the chosen work sheet items, and the revised items were distributed. The content of the work sheet differs for each company, but basic items include tube volt-

age, tube current, scan time, pitch, scan FOV, scan length, volume CT dose index ($CTDI_{vol}$), dose-length product (DLP), whether IR is used for scanning and 3D imaging, and the name and degree of IR protocol used. This questionnaire was prepared using Excel software (version 2013, Microsoft) and was distributed to each site.

The study started when the survey was sent on December 5, 2014, and results were collected by January 31, 2015. The study implementation period was 58 days.

Summary of the Collected Data on Fetal CT From the Sites

The frequency of usage for each piece of CT equipment and the protocol was summarized from the survey results. The CT parameters used at the sites were also compared among the results using the same protocol. The trend in results for the protocol that used the lowest dose and the protocol that used the highest dose was studied.

CT Exposure Evaluation Method

The minimum, one-fourth (25th percentile), median, three-fourths (75th percentile), and maximum values were obtained for the $CTDI_{vol}$, DLP, and scan length from the 139 fetal CT examinations collected in this 2015 study. The results were compared with the previous results in 2011 [5], and the changes over the 4 years were evaluated. In addition, the 75th percentile values of $CTDI_{vol}$ and DLP in this study were determined as the new DRL. The median value was compared for scan length.

Regarding usage of IR, the frequency of usage was studied and the difference in $CTDI_{vol}$ value was compared among cases with and without IR use.

Regarding tube voltage, the frequency of usage of 80, 100, and 120 kV was studied. The results were compared with those of the 2011 study [5]. In addition, the $CTDI_{vol}$ values for the frequently used voltages, 100 and 120 kV, were compared among the different protocols used. For statistical analysis of the data, an unpaired t test was used to test for significance (Excel version 2013, Microsoft).

Results
Response to Questions Addressed to the Obstetrician

Category of your hospital—The breakdown of the 22 sites was 13 university hospitals (59%), followed by six perinatal centers (27%), and three regional core hospitals (14%). However, there were inconsistencies in CT dose data on two sites. These sites were excluded and a total of 20 sites were used for analysis.

TABLE 1: Summary of 32 Fetal CT Protocols for Scanners Used at Each Survey Site

Manufacturer	Brand Name	Tube Voltage (kV)	Rotation Time (s)	Helical Pitch	Volume CT Dose Index (mGy)	Dose-Length Product (mGy·cm)	Iterative Reconstruction
GE Healthcare	Discovery 750HD ($n = 3$)	100 ($n = 4$)	0.4–1	0.5–1.4	0.5–9	18–353	ASiR ($n = 3$)
	LightSpeed 16 ($n = 1$)	120 ($n = 1$)					Veo ($n = 2$)
	LightSpeed VCT ($n = 1$)						
Siemens Healthcare	Sensation ($n = 2$)	120 ($n = 10$)	0.28–0.5	0.6–1.4	1.6–13	52–514	SAFIRE ($n = 4$)
	Definition ($n = 8$)						IRIS ($n = 1$)
Toshiba	Aquilion 16 ($n = 4$)	80 ($n = 1$)	0.3–0.75	0.8–1.5	1.8–27.5	55–943	AIDR3D ($n = 6$)
	Aquilion 64 ($n = 4$)	100 ($n = 4$)					
	Aquilion other ($n = 4$)	120 ($n = 12$)					QDS ($n = 1$)
	Aquilion ONE ($n = 3$)						
Philips Healthcare	iCT Elite ($n = 1$)	80 ($n = 1$)	0.4–0.75	0.6–0.9	1.6–7.9	70–281	IMR SoftTissue ($n = 1$)
	iCT ($n = 1$)	100 ($n = 1$)					iDose 4 ($n = 1$)
Summary of fetal CT protocols	$n = 32$	120 ($n = 23$)	0.28–0.75	0.5–1.5	0.5–27.5	18–943	Hybrid iterative reconstruction ($n = 17$)
		100 ($n = 9$)					Full iterative reconstruction ($n = 2$)

Note—ASiR = adaptive statistical iterative reconstruction, SAFIRE = sinogram-affirmed iterative reconstruction, IRIS = iterative reconstruction in image space, AIDR3D = adaptive iterative dose reduction 3D, QDS = quantum denoising software, IMR = iterative model reconstruction.

Specific written consent for fetal CT—Sixteen sites (80%) obtained specific written consent for conducting fetal CT.

Number of fetal CT examinations conducted in the past 3 years and 9 months—The number of cases per site during this time period ranged from one to 24 and there were 139 cases in total.

The range of and mean gestational week when CT was conducted—The range was 17–36 weeks' gestation, and the mean (± SD) was 30.1 ± 3.1 weeks.

Knowledge of the previous study report (2011), and whether the protocol has been changed—Six sites changed their protocol on the basis of the 2011 DRL (30%). Seven sites (35%) each answered that the study results did not affect their protocol or they did not know about the 2011 DRL.

Whether diagnostic ability decreased because of protocol change—No sites that changed their protocol answered that diagnostic ability decreased by lowering the dose.

Use of sedation on fetus during fetal CT—Two sites (10%) used sedation when conducting fetal CT, but the remaining 18 sites (90%) did not use sedation. One site that used sedation answered "walking, use of Diazepam in some cases," and the other site did not give a detailed response.

Knowledge of an approximate fetal CT radiation dose at own site—Obstetricians at 17 sites (85%) answered that they knew the approximate fetal CT radiation dose at their own site.

Summary of Collected Data on Fetal CT From Each Site

Table 1 summarizes the survey results about the 32 CT protocols used by the sites for each scanner manufacturer. The most common scanner manufacturer among the survey sites was Toshiba; however, no obvious difference of parameter setting was identified among CT vendors.

There was a wide range of radiation doses as measured by $CTDI_{vol}$ and DLP, and the lowest scanning condition was a $CTDI_{vol}$ of 0.5 mGy with the full IR method (Veo, GE Healthcare), even though full IR was used for only 10% of the protocols. This is somewhat surprising, because the maximum values of $CTDI_{vol}$ and DLP (27.5 mGy and 943 mGy·cm, respectively) were 50 times as large as the minimum settings (0.5 mGy and 18 mGy·cm, respectively). Approximately

68% of CT protocols were performed using a tube voltage of 120 kV.

CT Exposure Evaluation

Among the 139 fetal CT examinations performed at the study sites during the study period, inquiries were made to the staff in charge of setting imaging protocols for each manufacturer regarding incomplete data submitted from the sites to recover and ensure consistency in the data. However, inconsistencies in data on $CTDI_{vol}$ and DLP for 19 cases could still not be resolved. These data were excluded, and a total of 120 cases were used for analysis.

Evaluation and Change of Volume CT Dose Index, Dose-Length Product, and Scan Length

The comparison of values for $CTDI_{vol}$, DLP, and scan length in 2011 and 2015 is

TABLE 2: Comparison of Volume CT Dose Index ($CTDI_{vol}$), Dose-Length Product (DLP), and Scan Length Between 2011 and 2015

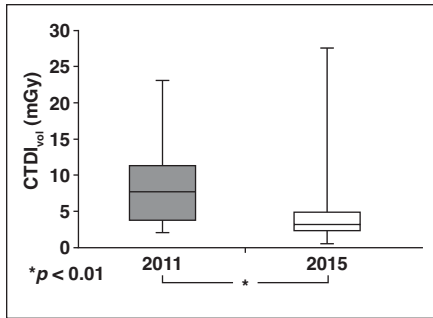| Measurement	$CTDI_{vol}$ (mGy)[a]		DLP (mGy·cm)[a]		Scan Length (mm)[b]	
	2011	2015	2011	2015	2011	2015
Maximum	23.1	27.5	1025.6	943.5	476	520
75th percentile	11.3	4.9	382.6	176.4	356	341
Median	7.7	3.2	276.8	104.3	319	313
25th percentile	3.7	2.4	122.3	84.8	295	287
Minimum	2.1	0.5	69	18.3	190	133

[a]$p < 0.01$.
[b]$p > 0.05$.

Fig. 1—Boxplot of volume CT dose index (CTDI$_{vol}$) values in 2011 and 2015. Boxes denote ranges, lines in boxes denote medians, and vertical lines and whiskers denote 95% CIs.
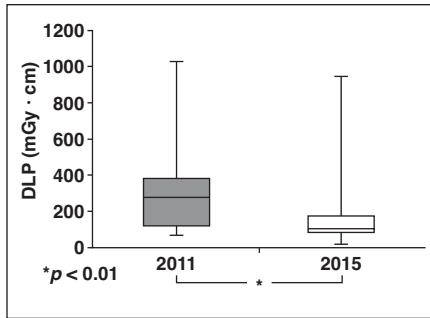

Fig. 2—Boxplot of dose-length product (DLP) values in 2011 and 2015. Boxes denote ranges, lines in boxes denote medians, and vertical lines and whiskers denote 95% CIs.
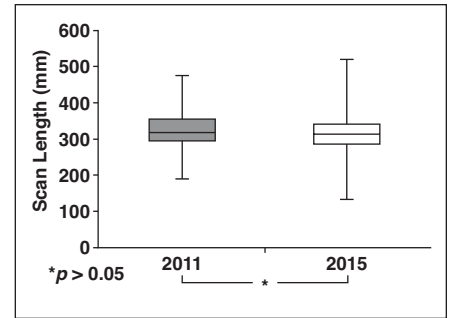

Fig. 3—Boxplot of scan length values in 2011 and 2015. Boxes denote ranges, lines in boxes denote medians, and vertical lines and whiskers denote 95% CIs.
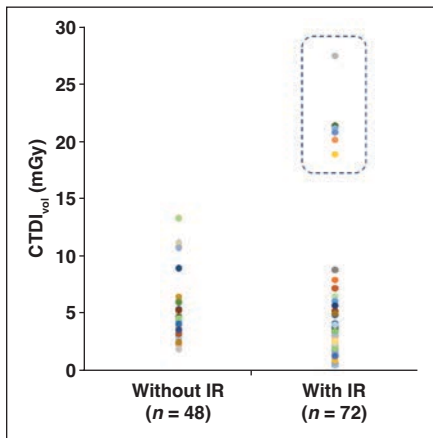

Fig. 4—Comparison of median volume CT dose index (CTDI$_{vol}$) between CT performed with and without iterative reconstruction (IR). If sites surrounded by dashed line are excluded, CTDI$_{vol}$ values for sites using IR are lower than for those that do not use IR, with statistically significant difference between groups ($p < 0.01$).
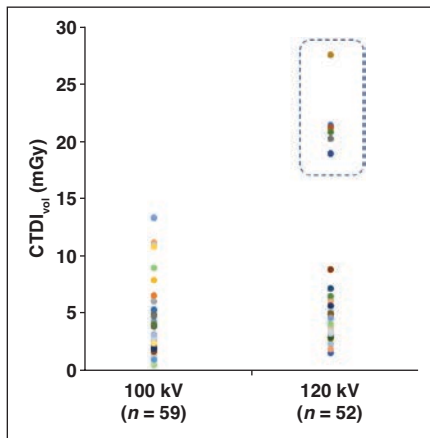

Fig. 5—Comparison of median volume CT dose index (CTDI$_{vol}$) values at 120 and 100 kV. In contrast to results for iterative reconstruction, results for tube current did not show significant difference in CTDI$_{vol}$ even when sites surrounded by dashed line were excluded.

shown in Table 2, and boxplots are shown in Figures 1–3. Compared with the study in 2011 ($n = 119$), the minimum, median, 75th percentile, and 25th percentile values of CTDI$_{vol}$ and DLP for the tabulated results in 2015 ($n = 120$) were lower, although some sites had a higher maximum value than that of the previous study. The 75th percentile value of CTDI$_{vol}$ that is the DRL for this study was 4.9 mGy, and this was 43% of the previous value of 11.3 mGy. During this period, a 57% reduction in the radiation dose was found (Fig. 1). Similar to CTDI$_{vol}$, the 75th percentile value for DLP was 176.4 mGy·cm, and this was 46% (about half) of the previous value of 382.4 mGy·cm. The differences were statistically significant ($p < 0.01$) (Fig. 2). On the other hand, the scan range was almost the same as in the previous study, and although the data included over 100 cases,

the median was different by only 6 mm, and the data were considered to be accurate. It was found that the decrease in DLP was not caused by a shortening of the length (Fig. 3).

In this study, 14 of 20 sites (70%) used IR. Among the 14 sites that used IR, six (43%) did not use the method at the beginning of

the study period but started to incorporate it during the study period. As shown in Figure 4, a comparison of CTDI$_{vol}$ between CT with IR ($n = 72$) and CT without IR ($n = 48$) shows that it is lower in the group that uses IR than the group that does not use IR, although one site had set a significantly higher radiation dose than the others (section surrounded by the dashed line in Fig. 4). If the site surrounded by the dashed line is excluded, the CTDI$_{vol}$ for sites using IR compared with those that do not use IR is statistically significantly lower ($p < 0.01$). The group that uses IR had a significantly lower radiation dose setting compared with the group that did not (Table 3).

Tube voltage was 120 kV in 52 cases, 100 kV in 59 cases, and 80 kV in nine cases, with 100 kV the most frequently used voltage. Six sites had the voltage fixed at 120 kV, whereas the other 14 sites used a tube voltage lower than 120 kV.

As with IR, comparison of CTDI$_{vol}$ values by tube current (120 vs 100 kV) showed that the median CTDI$_{vol}$ values for 120 and 100 kV were 3.3 and 2.5 mGy, respectively. As shown in Figure 5, the tube voltage was set at a significantly higher radiation dose in one

TABLE 3: Relationships Between Volume CT Dose Index (CTDI$_{vol}$) and Iterative Reconstruction (IR) and Between CTDI$_{vol}$ and Tube Voltage

Measurement	CTDI$_{vol}$ With and Without IR (mGy)[a]		CTDI$_{vol}$ at Different Tube Voltages (mGy)[b]	
	With IR	Without IR	120 kV	100 kV
Maximum	8.8	13.4	8.8	13.4
75th percentile	3.5	5	4.8	4.1
Median	2.5	3.3	3.3	2.5
25th percentile	2	3.2	3.2	2
Minimum	0.5	1.8	1.6	0.5

[a]$p < 0.01$.
[b]$p > 0.05$.

site in the group that used IR (section surrounded by a dashed line in Fig. 5). In contrast to the results for IR, the results for tube current did not show a significant difference in CTDI$_{vol}$ even when the site surrounded with the dashed line was excluded.

Discussion

From the response to the questions answered by the obstetricians, the following situation was revealed. In Japan, 86% of fetal CT examinations were performed at university hospitals or public perinatal centers that act as the center for medical care in that region. It is assumed that obstetricians and gynecologists at local clinics who detect short limbs by fetal ultrasound send a referral to obstetricians or fetal examination specialists for retesting by ultrasound with higher accuracy, and then the case is indicated for CT if necessary.

In Japan, 80% of the sites obtained specific written consent for fetal CT with informed consent from the parents regarding fetal radiation exposure.

The mean timing for the CT was 30.1 ± 3.1 weeks' gestation. This is thought to be the result of a recommendation by the leading academic research group on fetal CT in Japan, the Japan Forum of Fetal Skeletal Dysplasia, which recommends testing at around 30 weeks. This recommendation is based on several reasons, including the fact that the effect of radiation on the CNS is less of a concern during the third trimester of pregnancy [8] and that depiction of the skeletal structure is clearer compared with the early stages of pregnancy because of fetal growth. The result was almost the same as the previous study [5] (mean, 30.2 ± 2.6 weeks) with essentially no change. It is understandable that the sites that perform CT are actually following the recommendations of the Japan Forum of Fetal Skeletal Dysplasia.

Thirteen sites (65%) were aware of the DRL results from the 2011 study [5], and six sites (30%) had changed their protocol on the basis of the 2011 DRL. On the other hand, seven sites (35%) answered that they were not aware of the study results. DRL was proposed in the 1980s to optimize simple x-ray radiation dose and it was introduced as a method for optimizing CT radiation dose in the 1990s [7, 9]. It is considered that there is high awareness of DRL in the sites performing fetal CT, and DRL is correctly functioning as a regulatory pressure on the entire community as intended. No sites responded that a lower dose resulting from protocol

changes led to decreased diagnostic ability, and this further reinforces that these scanning conditions are appropriate.

It was revealed that 90% of sites did not sedate the fetus for fetal CT. In the previous survey, one site used pancuronium (Mioblock, MSD) to suppress fetal movement, but this response was not found in the current study. It is considered that sedation is not necessary for fetal CT.

Obstetricians at 17 sites (85%) knew the approximate fetal CT radiation dose of their site when they order the scan. According to a literature search, it has been reported in a past survey that only 16% of residents in a radiology department knew the radiation dose for abdominal CT [10]. The obstetricians at sites performing fetal CT may be aware of the dose because they are required to explain the dose to patients. This may be inaccurate because the specific number was not asked, but compared with past reports, obstetricians who are involved in fetal CT are considered to have a fairly high awareness of CT exposure.

This study has revealed that since the 2011 study [5], the DRL for fetal CT in Japan has been reduced by half, a result that was statistically significant. This may be due to three factors. One is the first-ever proposal of fetal CT DRL in Japan from the study results in 2011. The results were widely reported at fetal CT forums and research groups that were active in performing fetal CT. A total of 65% of the sites studied in this analysis answered that they were aware of the results, and, furthermore, 30% of sites responded that they had lowered their dose setting on the basis of the DRL of the previous study. This is the result of DRL fulfilling its correct function, and it could be evaluated as an extremely significant result for managing CT radiation exposure in Japan. It is considered that DRL should be studied every few years and, indeed, this study was conducted at the appropriate time. We should conduct another national survey in 3–4 years and confirm the decrease in DRL as a community.

The next factor is the decrease in dose due to widespread use of IR. In the previous 2011 study [5], only one site of 16 (6%) used IR, but in this study, there was a significant increase with 14 of 20 sites (70%) using IR. This is considered to be due to the recent recognition of IR in all CT scans, including those of children [11] and adults, and the experience of the scanner, who can easily enhance image quality by changing the console setting. Therefore, among the 14 sites that

used IR, the fact that six sites (43%) did not use IR at the beginning of the study but introduced IR later during the study period is considered to be the result of recognizing IR's usefulness in fetal CT.

The site that performs scans with the lowest exposure (CTDI$_{vol}$, 0.5 mGy) in this study does not use hybrid type IR but has introduced full IR (Veo, GE Healthcare) to aim for lower exposure. There are only a few reports on using full IR for fetal CT [12], but a decrease in fetal CT radiation dose would be possible if the full IR method becomes widespread, leading to a further decrease in DRL throughout Japan.

Similarly, this study found that many sites used low tube voltage. No significant difference in CTDI$_{vol}$ was found between different protocols using 120 or 100 kV, but the use of low tube voltage at these sites may be the result of awareness of lowering exposure and an adjustment to avoid an increase in unnecessary tube current. This is thought to be due to a change in techniques and awareness among the technicians in charge of CT machines in the clinical field.

In this way, radiation exposure of fetal CT has been optimized, but as shown in Figures 4 and 5, there are still sites with conditions leading to high radiation doses, and further education on DRL is required.

On the other hand, a limitation of this and previous studies was that only the radiation dose to set DRL was studied, and we did not collect data on image quality. Focusing on decreasing the dose may lead to a failure to maintain sufficient diagnostic quality for images. Goske et al. [13] have published their thoughts regarding the diagnostic reference range as a method to maintain both an appropriate radiation dose management for CT and diagnostic image quality. They suggest that the upper limit for radiation exposure should be the 75th percentile value and the lower limit should be the 25th percentile value to maintain image quality, and the appropriate scan condition should fall within this range. If this is applied to the results of this study, the appropriate dose for fetal CT would be a CTDI$_{vol}$ between 2.5 and 5 mGy (median, 3 mGy). In cases without full IR, this range for diagnostic reference range is considered to be appropriate.

A significant reduction in radiation exposure is possible if fetal CT is used only for observation of skeletal structure of the fetus, but it is necessary for each medical institution to consider the characteristics of IR for their fa-

cility's CT equipment and to perform a CT examination with sufficient quality for diagnosis.

In summary, since the previous DRL survey was conducted [5], the original objective and role for DRL that the International Commission on Radiological Protection [14] had proposed has been sufficiently reached. In addition, widespread use of IR and low tube voltage has helped in managing the radiation dose throughout Japan.

The objective of CT is to deliver an accurate diagnosis when skeletal dysplasia is suspected after careful fetal ultrasound testing and to determine the strategy for perinatal patient care. From this study, it was heartening to find that 85% of obstetricians who order CT scans were aware of the approximate CT radiation dose at their site.

We intend to conduct another survey in 4 years to confirm whether there is a further decrease in DRL. In addition, compared with 2011, there is concern that image quality may have been affected by the decrease in dose. Ideally, the next study would also include an evaluation of image quality.

Acknowledgments

References

1. Bonafe L, Cormier-Daire V, Hall C, et al. Nosology and classification of genetic skeletal disorders: 2015 revision. *Am J Med Genet A* 2015; 167A:2869–2892
2. Schumacher R, Seaver LH, Spranger J. Introduction. In: Schumacher R, Seaver LH, Spranger J, eds. *Fetal radiology, a diagnostic atlas*, 1st ed. Berlin, Germany: Springer, 2004:1–2
3. Toru HS, Nur BG, Sanhal CY. Perinatal diagnostic approach to fetal skeletal dysplasias: six years experience of a tertiary center. *Fetal Pediatr Pathol* 2015; 34:287–306
4. Miyazaki O, Nishimura G, Sago H, et al. Prenatal diagnosis of fetal skeletal dysplasia with 3D CT. *Pediatr Radiol* 2012; 42:842–852
5. Miyazaki O, Sawai H, Murotsuki J, et al. Nationwide radiation dose survey of computed tomography for fetal skeletal dysplasias. *Pediatr Radiol* 2014; 44:971–979
6. Brady Z, Framanauskas F, Cain TM, et al. Assessment of paediatric CT dose indicators for the purpose of optimization. *Br J Radiol* 2012; 85:1488–1498
7. Hopkins KL, Pettersson DR, Koudelka CK, et al. Size appropriate radiation doses in pediatric body CT: a study of regional community adoption in the United States. *Pediatr Radiol* 2013; 43:1128–1135
8. ACOG Committee on Obstetric Practice. ACOG committee opinion: number 299, September 2004 (replaces no. 158, September 1995)—guidelines for diagnostic imaging during pregnancy. *Obstet Gynecol* 2004; 104:647–651
9. Thomas KE. CT utilization: trends and developments beyond the United States' borders. *Pediatr Radiol* 2011; 41(suppl 2):562–566
10. Divrik Gökçe S, Gökçe E, Coşkun M. Radiology residents' awareness about ionizing radiation doses in imaging studies and their cancer risk during radiological examinations. *Korean J Radiol* 2012; 13:202–209
11. Haggerty JE, Smith EA, Kunisaki SM, et al. CT imaging of congenital lung lesions: effect of iterative reconstruction on diagnostic performance and radiation dose. *Pediatr Radiol* 2015; 45:989–997
12. Sekiguchi M, Miyazaki O, Wada S, et al. Case 13516: prenatal diagnosis of Pfeiffer syndrome type II using ultralow dose CT. EURORAD radiological case database website. www.eurorad.org/eurorad/case.php?id=13516. Published March 28, 2016. Accessed May 7, 2016
13. Goske MJ, Strauss KJ, Coombs LP, et al. Diagnostic reference ranges for pediatric abdominal CT. *Radiology* 2013; 268:208–218
14. Khong PL, Ringertz H, Donoghue V, et al.; ICRP. ICRP publication 121: radiological protection in paediatric diagnostic and interventional radiology. *Ann ICRP* 2013; 42:1–63

ORIGINAL ARTICLE

Serum NT-proCNP levels increased after initiation of GH treatment in patients with achondroplasia/hypochondroplasia

Takuo Kubota, Wei Wang, Kohji Miura, Hirofumi Nakayama, Keiko Yamamoto, Makoto Fujiwara, Yasuhisa Ohata, Makiko Tachibana, Taichi Kitaoka, Satoshi Takakuwa, Yoko Miyoshi, Noriyuki Namba and Keiichi Ozono

Department of Pediatrics, Osaka University Graduate School of Medicine, Osaka, Japan

Summary

Objective Serum amino-terminal propeptide of C-type natriuretic peptide (NT-proCNP) levels have been proposed as a biomarker of linear growth in healthy children. The usefulness of NT-proCNP in patients with achondroplasia (ACH)/hypochondroplasia (HCH) remains to be elucidated. The objective was to study whether serum NT-proCNP level is a good biomarker for growth in ACH/HCH and other patients of short stature.

Design This was a longitudinal cohort study.

Patients Sixteen children with ACH (aged 0·4–4·3 years), six children with HCH (2·7–6·3 years), 23 children with idiopathic short stature (ISS) (2·2–9·0 years), eight short children with GH deficiency (GHD) (2·9–6·8 years) and five short children born small for gestational age (SGA) (2·0–6·6 years). Patients with ACH/HCH received GH treatment for 1 year.

Measurements Serum NT-proCNP levels and height were measured.

Results NT-proCNP levels positively correlated with height velocity in these short children ($P < 0.05$, $r = 0.27$). NT-proCNP levels inversely correlated with age in children with ISS alone ($P < 0.01$, $r = -0.55$). Serum NT-proCNP levels in patients with ACH/HCH were increased 3 months following the initiation of GH treatment ($P < 0.05$). Height SDS gain during GH treatment for 1 year was positively correlated with the changes in NT-proCNP levels after the initiation of GH ($P < 0.01$, $r = 0.72$).

Conclusion Serum NT-proCNP levels may be a good biomarker to indicate the effect of GH treatment on growth in patients with ACH/HCH at least in the first year and height velocity in short stature patients.

Correspondence: Takuo Kubota, Department of Pediatrics, Osaka University Graduate School of Medicine, 2-2 Yamadaoka, Suita, Osaka 565-0871, Japan. Tel.: +81 6 6879 3932; Fax: +81 6 6879 3939; E-mail: tkubota@ped.med.osaka-u.ac.jp

Introduction

C-type natriuretic peptide (CNP) has been shown to be a critical determinant of body height and length.[1,2] Studies in genetically modified mice have revealed that defects of the genes coding for CNP and natriuretic peptide receptor 2 (Npr2), the cognate receptor for CNP, result in dwarfism[3,4]: both the ligand and its receptor are expressed in the growth plate as well as in other tissues.[5] In humans, loss-of-function mutations in the NPR2 gene cause an autosomal recessive skeletal dysplasia known as acromesomelic dysplasia, Maroteaux type (AMDM) (OMIM #602875), characterized by severe short stature with disproportionate shortened limbs. Heterozygous loss-of-function mutations in the gene have been recently identified in patients with idiopathic short stature (ISS).[6,7]

In contrast, overproduction of CNP in transgenic mice gives rise to excessive growth[8] and a similar phenotype is observed in patients with the overexpression of CNP due to chromosomal translocations.[9,10] We have established the disease entity of a heterozygous gain-of-function mutation in the NPR2 gene in a family with tall stature (OMIM #615923), which was replicated in mice with overexpression of the activating mutation in cartilage.[11] Functional analyses demonstrated that the gain-of-function mutation increases maximal enzymatic velocity and blocks desensitization of NPR2.[12] Two additional families with tall stature have been described that harbour gain-of-function mutations in the NPR2 gene.[13,14] These human and mouse genetic studies have shed light on the role of the CNP and NPR2 signalling pathway in determining growth and height.

Achondroplasia (ACH) (OMIM #100800) is the most common form of short-limb dwarfism in humans, affecting more than 250 000 individuals worldwide.[15] ACH and the milder form, hypochondroplasia (HCH) (OMIM #146000), occur because of constitutively active mutations in the fibroblast growth factor receptor 3 (FGFR3) gene, which influence the proliferation and differentiation of chondrocytes in growth plates. GH treatment improves height velocity at least during the first year and is approved in Japan for ACH and HCH patients with height standard deviation scores (SDS) below − 3·0 SD.[16–20] However, a biomarker to predict growth stimulated by GH treatment remains to be established.

The amino-terminal propeptide of CNP (NT-proCNP) is an equimolar product of CNP biosynthesis[21] and is more easily measured in serum because of its longer half-life compared to CNP.[22,23] Serum NT-proCNP levels have been recently reported to correlate with height velocity and change with age in healthy children.[23,24] In addition, serum NT-proCNP levels have been proposed as a novel biomarker of growth during GH treatment in patients with ISS and GH deficiency (GHD),[25,26] although age-associated changes in these levels have not been proven in ISS patients. In the current study, we determined the association of serum NT-proCNP levels with age in ISS patients and the relationship between response to GH treatment and height gain in patients with ACH/HCH.

Subjects and methods

Subjects

This study included 58 prepubertal patients who attended Osaka University Hospital, Osaka, Japan, from January 2009 through December 2013 and who were diagnosed with ACH, HCH, ISS, GH-deficient short stature and short stature born small for gestational age (SGA). Patients treated with GH and other drugs related to growth before and at the first visit were excluded. The diagnostic criteria for ACH included short stature, shortened limbs, abnormal facial features (prominent forehead, nasal root depression, mid-face hypoplasia and mandibular protrusion), an enlarged head size, and trident hands as clinical signs, and thick and short long bones, metaphyseal cupping, bullet-shaped vertebra, fibula that are longer than the tibia, decreased distance of lumbar spine pedicles, a large cranial base yet with small facial bones, a small ischial notch and a small cavity of the lesser pelvis as radiographic signs.[27] An ACH patient with a traumatic acute epidural haematoma was excluded. Patients with HCH were diagnosed based on clinical and radiographic findings similar to but milder than those with ACH and the p.N540K mutation in the *FGFR3* gene on genetic analysis. The diagnostic criteria for GH-deficient short stature were the following: proportional short children with height SDS below −2·0, GH peak values less than 4·29 µg/l in two different provocation tests measured using a chemiluminescent enzyme immunoassay (Beckman Coulter) and no clinical and biochemical evidence of other disorders. The diagnostic criteria for short stature born SGA were the following: both birth length and weight for gestational age less than the 10th percentile, either birth length or weight SDS for gestational age less than −2·0, height SDS less than −2·0 at the age of 2 years and no clinical or biochemical findings of other disorders including GHD. Patients with ISS exhibited a proportional short stature with height SDS below −2·0 and lacked any features and findings of disorders with short stature, including GHD, other endocrine disorders, short stature born SGA, skeletal dysplasias, malformation syndromes and malnutrition.

Sixteen patients with ACH (8 boys, 8 girls) were included in the current study. Gene analysis in 13 of these patients revealed that all had p.G380R mutation in *FGFR3*. Median age and height SDS in patients with ACH was 3·1 years (minimum 0·4, 25th percentile 2·9, 75th percentile 3·4, maximum 4·3) and −5·2 (interquartile range: −5·7 to −4·2), respectively. Six patients with HCH (3 boys, 3 girls) were included: median age 3·2 years (2·7, 2·9, 4·1, 6·3) and height SDS −3·3 (−4·3 to −2·3). GH treatment is approved in Japan for both patients with ACH and HCH over the age of 3 with height SDS below −3·0, at a dose of 0·35 mg/kg/week (50 µg/kg/day). Fifteen of the ACH/HCH patients (11 ACH; 4 HCH) with GH treatment and 1-year follow-up were included where serum NT-proCNP levels were examined after the initiation of GH treatment. Mean height SDS increased significantly from −4·8 (1·0) [mean (SD)] to −4·3 (1·2) after GH treatment for 1 year. The remaining seven patients with ACH/HCH were not included for studies after the initiation of GH treatment due to the following reasons: two patients with ACH and two patients with HCH did not meet the criteria for GH treatment; two patients with ACH moved to a new location and were not followed up; one patient with ACH had GH treatment for a very short time. Twenty-three patients with ISS (14 boys, 9 girls) were included in this study: median age 5·4 years (2·2, 3·7, 6·7, 9·0) and height SDS −2·5 (−2·6 to −2·2). The study also included eight GH-deficient short patients (all boys) [median age 4·5 years (2·9, 4·0, 5·4, 6·8) and height SDS −2·9 (−3·1 to −2·5)] and five short stature born SGA patients (2 boys, 3 girls) [median age 3·0 years (2·0, 2·3, 5·8, 6·6) and height SDS −2·4 (−3·1 to −2·2)].

Measurements

Laboratory measurements included serum levels of alkaline phosphatase (AP) (reference range: 134–359 U/l for adults) and IGF-1 [for reference range see[28]]. Serum NT-proCNP levels were measured using an ELISA method (Biomedica, Austria). Measurement of serum NT-proCNP levels was approved by the Institutional Review Board at Osaka University Hospital, and written informed consent was obtained from parents or guardians of the patients.

Statistical analysis

Data were analysed by Wilcoxon rank–sum test, regression analysis, paired *t*-test or Smirnov–Grubbs' test using JMP (SAS Institute, Cary, NC, USA) and R (GNU General Public License, Free Software Foundation, Inc., Boston, MA, USA) statistical software.

Results

Serum NT-proCNP levels in patients with ACH/HCH, ISS, GHD and short stature born SGA

Serum NT-proCNP levels were positively correlated with height velocity in prepubertal patients with short stature (Fig. 1a), implying that the serum NT-proCNP level can be a biomarker of growth in short children independently of their pathogenesis. As the numbers of patients with GHD and short stature born SGA were small, we subsequently focused on patients with
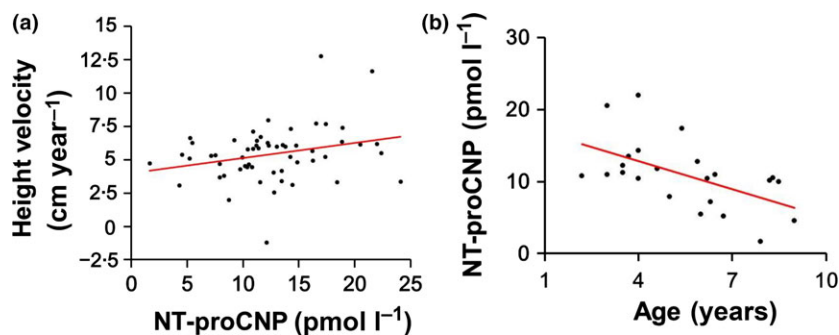
Fig. 1 Serum NT-proCNP levels in patients with short stature. (a) Height velocity positively correlates with serum NT-proCNP levels in prepubertal short children with ACH, HCH, ISS, GHD and SGA ($P < 0.05$, $r = 0.27$, $n = 58$). (b) Serum NT-proCNP levels were negatively correlated with age in ISS children ($P < 0.01$, $r = -0.55$, $n = 23$).

ACH/HCH and ISS. On division of ISS patients into two subgroups by the median age of the group, serum NT-proCNP levels were higher in those <5·4 years of age (median [interquartile range]: 12·0 [10·8–16·6]) compared to those >5·4 years of age (10·0 [5·2–10·5]). Consistently, serum NT-proCNP levels were negatively correlated with age in ISS children (Fig. 1b). Unlike in ISS patients, there was no obvious correlation between serum NT-proCNP levels and age in patients with ACH/HCH, probably due to small distribution of age (data not shown). In addition, serum NT-proCNP levels in patients with ACH/HCH ($n = 15$; median [interquartile range], 12·8 [9·2–16·3]) and ACH alone (11; 12·8 [9·2–16·3]) were similar to those in patients with ISS (5; 12·2 [11·1–17·0]) at 3 years of age, implying that CNP production is comparable between patients with ACH/HCH and ISS, at least at that age, even though there was a difference in height SDS between ACH/HCH or ACH alone and ISS.

Association of serum NT-proCNP levels with growth during GH treatment in patients with ACH/HCH

Serum NT-proCNP levels were assessed in patients with ACH/HCH before and after the initiation of GH treatment to determine the effect of GH on serum NT-proCNP levels. Serum NT-proCNP levels were increased in patients with ACH/HCH 3 months following the initiation of GH, which is consistent with increments in serum IGF-1 SDS and AP levels induced by GH (Fig. 2a–c). To test whether serum NT-proCNP levels can be a good biomarker of the effect of GH treatment on growth in

patients with ACH/HCH, we examined the association of an increase in serum NT-proCNP levels following the initiation of GH treatment with height gain after 1 year of treatment. When patients with ACH/HCH were divided into subgroups with respect to their increase in serum NT-proCNP levels 3 months after the initiation of GH (lower and upper subgroups), the increase in height SDS was larger after 12 months' treatment in the subgroup with the higher increase in serum NT-proCNP levels (Figure 3a). In addition, the change in height SDS 1 year after GH treatment was positively correlated with fold change in NT-proCNP 3 months after the treatment (Fig. 3b). The association of NT-proCNP levels with height gain may differ between patients with ACH and HCH, as growth response to GH treatment in patients with HCH has been reported to be larger than that in patients with ACH.[29] We therefore examined this association in patients with ACH alone. The results in these patients were similar to those in patients with ACH/HCH; that is, the increase in serum NT-proCNP levels was positively correlated with height gain following the initiation of GH treatment (Fig. 4a, b). On the other hand, the association of height gain with an increment in serum IGF-1 SDS or AP levels following the initiation of GH treatment was not observed in patients with ACH/HCH (Figure 3c–f) or ACH alone (Fig. 4c–f), although these markers increased after GH treatment.

Discussion

Our study confirms that serum NT-proCNP levels are positively correlated with height velocity in children with short stature. In
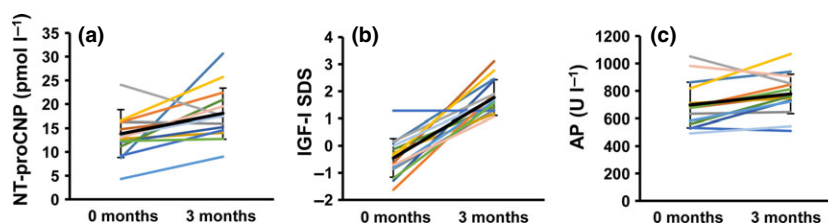
Fig. 2 Increase in serum NT-proCNP levels, IGF-1 SDS and AP levels of patients with ACH/HCH following the initiation of GH treatment. (a) NT-proCNP ($P < 0.05$), (b) IGF-1 SDS ($P < 0.01$), (c) and AP ($P < 0.05$) levels were increased in patients with ACH ($n = 11$)/HCH ($n = 4$) 3 months after the initiation of GH treatment compared to prior to treatment. Bold lines show mean ± SD. ACH, achondroplasia; AP, alkaline phosphatase; HCH, hypochondroplasia; mo, month; NT-proCNP, amino-terminal propeptide of C-type natriuretic peptide; SDS, standard deviation score.
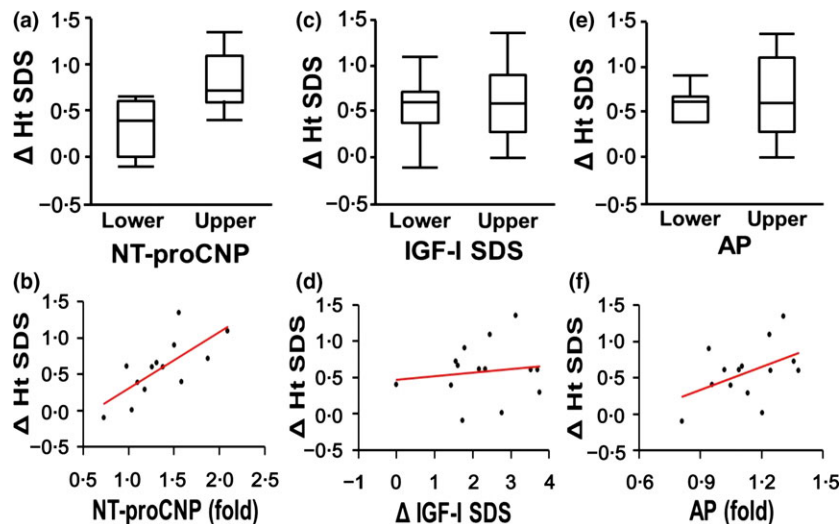
Fig. 3 Association of Δ Ht SDS with serum NT-proCNP level, IGF-1 SDS and AP level following the initiation of GH treatment in patients with ACH ($n = 10$)/HCH ($n = 4$). Upper panels show box plots and lower panels correlation. (a) When patients were divided into subgroups [lower ($n = 7$) and upper ($n = 7$)] according to a 35% cut-off increase in NT-proCNP level 3 months after starting GH treatment, Δ Ht SDS was significantly ($P < 0·05$) higher 1 year after GH treatment in the upper compared to the lower subgroup. (b) Δ Ht SDS 1 year after GH treatment was positively correlated with fold change of serum NT-proCNP 3 months after GH treatment ($P < 0·01$, $r = 0·72$, $n = 13$). (c) When patients were divided into subgroups [lower ($n = 7$) and upper ($n = 7$)] according to a 1·7 cut-off increase in IGF-1 SDS 3 months after starting GH treatment, Δ Ht SDS was comparable in the subgroups. (d) Δ Ht SDS 1 year after GH treatment was not correlated with Δ serum IGF-I SDS 3 months after GH treatment. (e) When patients were divided into subgroups [lower ($n = 7$) and upper ($n = 7$)] according to a 10% cut-off increase in serum AP 3 months after starting GH treatment, Δ Ht SDS was comparable in the subgroups. (f) Δ Ht SDS 1 year after GH treatment was not significantly correlated with fold change of serum AP 3 months after GH treatment. ACH, achondroplasia; AP, alkaline phosphatase; HCH, hypochondroplasia; NT-proCNP, amino-terminal propeptide of C-type natriuretic peptide; SDS, standard deviation score.
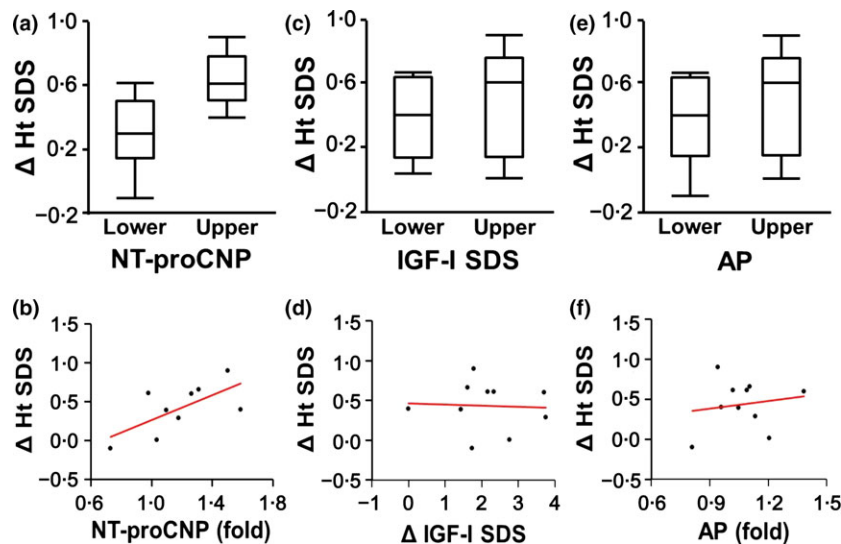
Fig. 4 Association of Δ Ht SDS with serum NT-proCNP level, IGF-1 SDS and AP level following the initiation of GH treatment in patients with ACH ($n = 10$). Upper panels show box plots and lower panels correlation. (a) When patients were divided into subgroups [lower ($n = 5$) and upper ($n = 5$)] according to a 20% cut-off increase in NT-proCNP level 3 months after starting GH treatment, Δ Ht SDS was significantly($P < 0·05$) higher 1 year after GH treatment in the upper compared to the lower subgroup. (b) Δ Ht SDS 1 year after GH treatment was positively correlated with fold change of serum NT-proCNP 3 months after GH treatment ($P < 0·05$, $r = 0·67$, $n = 10$). (c) When patients were divided into subgroups [lower ($n = 5$) and upper ($n = 5$)] according to a 2·2 cut-off increase in IGF-1 SDS 3 months after starting GH treatment, Δ Ht SDS was comparable in the subgroups. (d) Δ Ht SDS 1 year after GH treatment was not correlated with Δ serum IGF-I SDS 3 months after GH treatment. (e) When patients were divided into subgroups [lower ($n = 5$) and upper ($n = 5$)] according to a 7% cut-off increase in serum AP 3 months after starting GH treatment, Δ Ht SDS was comparable in the subgroups. (f) Δ Ht SDS 1 year after GH treatment was not significantly correlated with fold change of serum AP 3 months after GH treatment. ACH, achondroplasia; AP, alkaline phosphatase; HCH, hypochondroplasia; NT-proCNP, amino-terminal propeptide of C-type natriuretic peptide; SDS, standard deviation score.

addition, we showed the increase in NT-proCNP following the initiation of GH treatment in patients with ACH/HCH was significantly correlated with the gain in height velocity. A similar study has reported that changes in NT-proCNP levels are positively correlated with growth velocity in the first year of GH treatment in ISS patients.[25] Therefore, CNP production in response to GH treatment may be maintained even in chondrocytes carrying the *FGFR3* mutation.

Serum NT-proCNP levels were increased 3 months following the initiation of GH treatment in patients with ACH/HCH, as well as serum IGF-1 SDS and AP levels, indicating that CNP is produced in response to GH and/or IGF-1 stimulation in these patients. This is in agreement with previous reports on the effect of GH treatment in ISS and GHD patients.[25,26] However, the mechanisms by which GH and/or IGF-1 stimulate CNP expression are unclear. Although CNP expression *in vitro* is regulated by TGF-β and receptor tyrosine kinase growth factors in a cell/tissue-specific and sometimes species-specific manner, crucial details of the regulatory pathways that lead to suppression or induction of CNP transcription remain unknown.[30] Our *in vivo* data suggest that CNP production may be upregulated, at least in part, by the endocrine GH and IGF-1 system.

We also found that an increase in serum NT-proCNP levels by GH treatment is positively correlated with the increase in height velocity during treatment in patients with ACH/HCH. Serum IGF-1 SDS and AP levels were also increased but they were not correlated, which is consistent with the results of ISS patients in previous studies in terms of serum IGF-1 levels.[25,31] A previous report did not show a correlation in patients with ACH.[17] With respect to serum levels of AP, a marker of bone formation, a study of patients with HCH treated with GH found no correlation between height gain and increase in osteocalcin, another bone formation marker,[19] which is consistent with the AP data in the current study. These results indicate that serum NT-proCNP levels may be a useful marker to indicate the effect of GH treatment on growth in patients with ACH/HCH. Moreover, the positive correlation between height velocity and NT-proCNP after GH treatment may indicate that CNP production promotes height gain in patients with ACH/HCH, which has been reported in a mouse ACH model.[32]

Serum NT-proCNP levels were negatively correlated with age in prepubertal children with ISS and positively correlated with height velocity in short children with ACH/HCH, ISS, GHD and short stature born SGA. The correlation of NT-proCNP levels with height velocity in each of the conditions was not proven, probably due to the small numbers in each group (data not shown). Regarding ISS patients, serum NT-proCNP levels are likely to be positively correlated with height velocity due to the decline of height velocity with age in prepubertal children. These results are consistent with those in healthy children and patients with ACH.[24,33] This indicates that serum NT-proCNP levels may be a biomarker of growth velocity in patients with ISS, and presumably other short children with ACH, HCH, GHD and short stature born SGA.

Serum NT-proCNP levels were comparable in ISS patients to those in patients with ACH/HCH and ACH alone at 3 of years age despite a difference in height SDS. This was not studied at other ages because GH treatment is generally initiated in most patients with ACH/HCH at 3 years of age. Furthermore, comparable NT-proCNP SDS has been described for patients with ACH and HCH despite a difference in height SDS.[33] These results indicate that NT-proCNP levels might not reflect height SDS at the time of measurement. On the other hand, NT-proCNP SDS has been reported to be elevated in patients with ACH and HCH compared to the reference population.[33] The difference in NT-proCNP levels in ACH may be due to a difference in NT-proCNP assay and/or a difference in the age of patients with ACH. Whatever, it is noteworthy that CNP production is not reduced in patients with ACH even though chondrocytes carry the *FGFR3* mutation and develop in an abnormal pattern.

Our study has some limitations. First, the sample size is small. However, our results indicate that serum NT-proCNP levels are a biomarker of growth velocity in patients with ACH/HCH following the initiation of GH treatment. Secondly, we did not have a control group composed of healthy infants, as sampling from healthy children was not permitted from an ethical point of view.

In summary, our study revealed that serum NT-proCNP level is a biomarker of growth velocity in patients with ACH/HCH following the initiation of GH treatment. It is also suggested that serum NT-proCNP levels might be a biomarker of growth in ISS patients.

Acknowledgements

Grants

Disclosure summary

The authors have no conflicts to disclose.

References

1 Vasques, G.A., Arnhold, I.J.P. & Jorge, A.A.L. (2014) Role of the natriuretic peptide system in normal growth and growth disorders. *Hormone Research in Paediatrics*, **82**, 222–229.

2 Yasoda, A. & Nakao, K. (2010) Translational research of C-type natriuretic peptide (CNP) into skeletal dysplasias. *Endocrine Journal*, **57**, 659–666.

3 Chusho, H., Tamura, N., Ogawa, Y. *et al.* (2001) Dwarfism and early death in mice lacking C-type natriuretic peptide. *Proceedings of the National Academy of Sciences of the United States of America*, **98**, 4016–4021.

4 Tamura, N., Doolittle, L.K., Hammer, R.E. *et al.* (2004) Critical roles of the guanylyl cyclase B receptor in endochondral

ossification and development of female reproductive organs. *Proceedings of the National Academy of Sciences of the United States of America*, **101**, 17300–17305.

5 Potter, L.R., Abbey-Hosch, S. & Dickey, D.M. (2006) Natriuretic peptides, their receptors, and cyclic guanosine monophosphate-dependent signaling functions. *Endocrine Reviews*, **27**, 47–72.

6 Vasques, G.A., Amano, N., Docko, A.J. et al. (2013) Heterozygous mutations in natriuretic peptide receptor-B (NPR2) gene as a cause of short stature in patients initially classified as idiopathic short stature. *Journal of Clinical Endocrinology and Metabolism*, **98**, E1636–E1644.

7 Amano, N., Mukai, T., Ito, Y. et al. (2014) Identification and functional characterization of two novel NPR2 mutations in Japanese patients with short stature. *Journal of Clinical Endocrinology and Metabolism*, **99**, E713–E718.

8 Yasoda, A., Komatsu, Y., Chusho, H. et al. (2004) Overexpression of CNP in chondrocytes rescues achondroplasia through a MAPK-dependent pathway. *Nature Medicine*, **10**, 80–86.

9 Moncla, A., Missirian, C., Cacciagli, P. et al. (2007) A cluster of translocation breakpoints in 2q37 is associated with overexpression of NPPC in patients with a similar overgrowth phenotype. *Human Mutation*, **28**, 1183–1188.

10 Bocciardi, R., Giorda, R., Buttgereit, J. et al. (2007) Overexpression of the C-type natriuretic peptide (CNP) is associated with overgrowth and bone anomalies in an individual with balanced t (2;7) translocation. *Human Mutation*, **28**, 724–731.

11 Miura, K., Namba, N., Fujiwara, M. et al. (2012) An overgrowth disorder associated with excessive production of cGMP due to a gain-of-function mutation of the natriuretic peptide receptor 2 gene. *PLoS ONE*, **7**, e42180.

12 Robinson, J.W., Dickey, D.M., Miura, K. et al. (2013) A human skeletal overgrowth mutation increases maximal velocity and blocks desensitization of guanylyl cyclase-B. *Bone*, **56**, 375–382.

13 Miura, K., Kim, O.-H., Lee, H.R. et al. (2014) Overgrowth syndrome associated with a gain-of-function mutation of the natriuretic peptide receptor 2 (NPR2) gene. *American Journal of Medical Genetics Part A*, **164A**, 156–163.

14 Hannema, S.E., van Duyvenvoorde, H.A., Premsler, T. et al. (2013) An activating mutation in the kinase homology domain of the natriuretic peptide receptor-2 causes extremely tall stature without skeletal deformities. *Journal of Clinical Endocrinology and Metabolism*, **98**, E1988–E1998.

15 Horton, W.A., Hall, J.G. & Hecht, J.T. (2007) Achondroplasia. *Lancet*, **370**, 162–172.

16 Tanaka, H., Kubo, T., Yamate, T. et al. (1998) Effect of growth hormone therapy in children with achondroplasia: growth pattern, hypothalamic-pituitary function, and genotype. *European Journal of Endocrinology*, **138**, 275–280.

17 Hertel, N.T., Eklöf, O., Ivarsson, S. et al. (2005) Growth hormone treatment in 35 prepubertal children with achondroplasia: a five-year dose-response trial. *Acta Paediatrica*, **94**, 1402–1410.

18 Horton, W.A., Hecht, J.T., Hood, O.J. et al. (1992) Growth hormone therapy in achondroplasia. *American Journal of Medical Genetics*, **42**, 667–670.

19 Pinto, G., Cormier-Daire, V., Le Merrer, M. et al. (2014) Efficacy and safety of growth hormone treatment in children with hypochondroplasia: Comparison with an historical cohort. *Hormone Research in Paediatrics*, **86**, 355–363.

20 Rothenbuhler, A., Linglart, A., Piquard, C. et al. (2012) A pilot study of discontinuous, insulin-like growth factor 1-dosing growth hormone treatment in young children with FGFR3 N540K-mutated hypochondroplasia. *Journal of Pediatrics*, **160**, 849–853.

21 Wu, C., Wu, F., Pan, J. et al. (2003) Furin-mediated processing of pro-C-type natriuretic peptide. *Journal of Biological Chemistry*, **278**, 25847–25852.

22 Prickett, T.C., Yandle, T.G., Nicholls, M.G. et al. (2001) Identification of amino-terminal pro-C-type natriuretic peptide in human plasma. *Biochemical and Biophysical Research Communications*, **286**, 513–517.

23 Prickett, T.C., Lynn, A.M., Barrell, G.K. et al. (2005) Amino-terminal proCNP: a putative marker of cartilage activity in postnatal growth. *Pediatric Research*, **58**, 334–340.

24 Olney, R.C., Permuy, J.W., Prickett, T.C.R. et al. (2012) Amino-terminal propeptide of C-type natriuretic peptide (NTproCNP) predicts height velocity in healthy children. *Clinical Endocrinology (Oxford)*, **77**, 416–422.

25 Xiao, Y., Dong, Z., Lu, W. et al. (2011) Measurement of amino-terminal propeptide of C-type natriuretic peptide in patients with idiopathic short stature or isolated growth hormone deficiency. *Journal of Pediatric Endocrinology and Metabolism*, **24**, 989–994.

26 Olney, R.C., Prickett, T.C.R., Yandle, T.G. et al. (2007) Amino-terminal propeptide of C-type natriuretic peptide and linear growth in children: effects of puberty, testosterone, and growth hormone. *Journal of Clinical Endocrinology and Metabolism*, **92**, 4294–4298.

27 Ozono, K., Namba, N., Kubota, T. et al. (2012) Pediatric aspects of skeletal dysplasia. *Pediatric Endocrinology Reviews*, **10**(Suppl 1), 35–43.

28 Isojima, T., Shimatsu, A., Yokoya, S. et al. (2012) Standardized centile curves and reference intervals of serum insulin-like growth factor-I (IGF-I) levels in a normal Japanese population using the LMS method. *Endocrine Journal*, **59**, 771–780.

29 Tanaka, N., Katsumata, N., Horikawa, R. et al. (2003) The comparison of the effects of short-term growth hormone treatment in patients with achondroplasia and with hypochondroplasia. *Endocrine Journal*, **50**, 69–75.

30 Sellitti, D.F., Koles, N. & Mendonça, M.C. (2011) Regulation of C-type natriuretic peptide expression. *Peptides*, **32**, 1964–1971.

31 Mortensen, H.B., Main, K., Michaelsen, K.F. et al. (1991) Predicting and monitoring of growth in children with short stature during the first year of growth hormone treatment. *Acta Paediatrica Scandinavica*, **80**, 1150–1157.

32 Lorget, F., Kaci, N., Peng, J. et al. (2012) Evaluation of the therapeutic potential of a CNP analog in a Fgfr3 mouse model recapitulating achondroplasia. *American Journal of Human Genetics*, **91**, 1108–1114.

33 Olney, R.C., Prickett, T.C.R., Espiner, E.A. et al. (2014) C-type natriuretic peptide (CNP) plasma levels are elevated in subjects with achondroplasia, hypochondroplasia, and thanatophoric dysplasia. *Journal of Clinical Endocrinology and Metabolism*, **100**, E355–E359.

DR TAICHI KITAOKA (Orcid ID : 0000-0002-3531-884X)

Safety and Efficacy of Treatment with Asfotase Alfa in Patients with Hypophosphatasia: Results from a Japanese Clinical Trial

Short title: Clinical Trial of Asfotase Alfa

Authors: Taichi Kitaoka[1], Toshihiro Tajima[2], Keisuke Nagasaki[3], Toru Kikuchi[3], Katsusuke Yamamoto[4], Toshimi Michigami[5], Satoshi Okada[6], Ikuma Fujiwara[7], Masayuki Kokaji[8], Hiroshi Mochizuki[9], Tsutomu Ogata[10], Koji Tatebayashi[11], Atsushi Watanabe[12], Shuichi Yatsuga[13], Takuo Kubota[1], Keiichi Ozono[1]

Affiliations: [1]Department of Pediatrics, Osaka University Graduate School of Medicine, Osaka, Japan [2]Department of Pediatrics, Hokkaido University School of Medicine, Sapporo, Japan [3]Division of Pediatrics, Department of Homeostatic Regulation and Development, Niigata University Graduate School of Medical and Dental Sciences, Niigata, Japan

[4]Department of Pediatric Nephrology and Metabolism, Osaka Medical Center and Research Institute for Maternal and Child Health, Osaka, Japan [5]Department of Bone and Mineral Research, Osaka Medical Center and Research Institute for Maternal and Child Health, Osaka, Japan [6]Department of Pediatrics, Hiroshima University Graduate School of Biomedical & Health Sciences, Hiroshima, Japan [7]Department of Pediatrics, Tohoku University School of Medicine, Miyagi, Japan, [8]Department of Pediatrics, Showa General Hospital, Tokyo, Japan [9]Division of Endocrinology and Metabolism, Saitama Children's Medical Center, Saitama, Japan [10]Department of Pediatrics, Hamamatsu University School of Medicine, Hamamatsu, Japan [11]Department of Pediatrics, Nagara Medical Center, Gifu, Japan [12]Division of Clinical Genetics, Nippon Medical School Hospital, Tokyo, Japan [13]Department of Pediatrics and Child Health, Kurume University School of Medicine, Fukuoka, Japan

Toshihiro Tajima's present affiliation is Jichi Children's Medical Center Tochigi, Tochigi, Japan

Toru Kikuchi's present affiliation is Department of Pediatrics, Saitama Medical University, Saitama, Japan

Correspondence: Keiichi Ozono, MD, PhD, 2-2 Yamada-oka, Suita, Osaka 565-0871, Japan,

Tel: +81-6-6879-3932, Fax: +81-6-6879-3939, Email: keioz@ped.med.osaka-u.ac.jp

report. The participating institutions are supported by the Japanese Health Authority and the

Ministry of Health, Labour and Welfare.

Abstract length: 246 words

Text length: 3311 words

No. of graphics: 6 (4 tables, 2 figures)

No. of references: 24

Supplementary information: Provided as separate file

Summary

Objective Hypophosphatasia (HPP) is a rare skeletal disease characterized by hypomineralization and low alkaline phosphatase activity. Asfotase alfa (AA) has been recently developed to treat HPP complications. This study evaluated its safety and efficacy in Japan.

Design Open-label, multicenter, prospective trial. Patients were enrolled in 11 hospitals from June 2014 to July 2015.

Patients Thirteen patients (9 females, 4 males) ages 0 days to 34 years at baseline were enrolled and treated with AA (2 mg/kg three times weekly subcutaneously in all but one patient). All had *ALPL* gene mutations. HPP forms were perinatal ($n = 6$), infantile ($n = 5$), childhood ($n = 1$), and adult ($n = 1$).

Measurements Safety determined from adverse events (AEs) and laboratory data was the primary outcome measure. Efficacy was assessed as a secondary outcome measure from overall survival, respiratory status, rickets severity, and gross motor development.

Results Injection site reactions were the most frequent AEs. Serious AEs possibly related to treatment were convulsion and hypocalcemia observed in a patient with the perinatal form. In addition, hypercalcemia and/or hyperphosphatemia was observed in three patients with the infantile form and a low-calcium and/or low-phosphate formula was given to these patients.

With respect to efficacy, all patients survived and the radiographic findings, developmental

milestones, and respiratory function improved.

Conclusion AA therapy improved skeletal, respiratory, and physical symptoms with a few

serious AEs in patients with HPP. Our results add support to the safety and efficacy of AA

therapy for HPP patients.

Introduction

Hypophosphatasia (HPP) is a rare skeletal disease caused by defects of the gene *ALPL*, which

encodes tissue-non-specific alkaline phosphatase (TNSALP). More than 300 mutations are

registered on the website edited by Prof. Monet E

(http://www.sesep.uvsq.fr/03_hypo_mutations.php). Impaired bone mineralization due to low

levels of alkaline phosphatase (ALP) activity is characteristic of HPP.[1,2] However, the

phenotype of HPP varies and is usually classified into six forms based on age at onset and

severity of clinical features: perinatal, benign pre-natal, infantile, childhood, adult, and

odonto forms.[1–7] The mutations leading to a complete loss of ALP enzyme activity are

generally associated with severe forms. In Japanese patients, c.1559delT is the most frequent

mutation and is often associated with severe forms.[8–11]

The prognosis associated with the most severe form of HPP is very poor, because such patients suffer from respiratory failure due to marked hypomineralization of bones. Advances in neonatal intensive care including respiratory and circulatory support have improved prognosis. However, patients with the severe form of HPP require highly effective therapy to survive because its associated survival rate has been reported to be 42% and 27% at the age of 1 and 5 years, respectively.[12] Enzyme replacement therapy using bone-targeting recombinant alkaline phosphatase (asfotase alfa: AA) has been developed and is expected to improve prognosis. A clinical trial of AA has reported it to be safe and effective for 10 patients with perinatal, infantile, and childhood HPP.[13,14] Moreover, a long-term study of AA demonstrated the improvement of mineralization, respiratory function, and survival rate in 37 patients with perinatal and infantile HPP compared to 48 historical controls.[12] However, more experience is needed to better establish its safety and efficacy. We therefore conducted an investigator-initiated clinical trial of AA in Japan to further evaluate its safety and efficacy.

Methods

Study design

The study design was devised by the authors at Osaka University with the assistance of Dr. Kiyoshi Okada (Medical Center for Translational and Clinical Research, Department of

Medical Innovation, Osaka University Hospital, Osaka, Japan). Dr. Keiichi Ozono acted as the coordinating investigator. Data on the safety and efficacy and the statistical analyses were monitored by Translational Research Informatics Center (Kobe, Japan). The protocol was approved by the local institutional review boards of the participating institutions. The study was conducted following Good Clinical Practice guidelines and adhered to the Declaration of Helsinki. Written informed consent was obtained from the parents of the patients except for an adult patient who gave informed consent himself. The trial was registered (NCT02456038, UMIN000014816, and HPPJEAP-01).

We studied the safety and efficacy of treatment with repeated subcutaneous (SC) injections of AA in patients with HPP in an open-label, single-arm, multicenter, investigator-initiated clinical study. The primary outcome measure was the safety of AA. Secondary outcome measures included overall survival, respiratory status, rickets severity, physical growth, and gross motor development. Patients were enrolled in 11 hospitals from June 2014 to July 2015 when AA received marketing approval in Japan.

Eligible patients included those of any age who had been already diagnosed with HPP, who had been already treated with AA outside of this clinical trial, or who had one or more features of HPP such as serum ALP activity below age-adjusted lower limits of normal, HPP related-findings, or positive genetic testing (*ALPL* mutations). All of the patients enrolled in the study, in fact, had mutations of the *ALPL* gene. Exclusion criteria included treatable forms

of rickets, hypocalcemia, hypophosphatemia, or treatment with bisphosphonates. Detailed

inclusion/exclusion criteria are provided as Supplementary Information (Supplementary

Methods).

Clinical assessments including physical growth, vital signs, and laboratory data were

collected at baseline, every 4 weeks until 24 weeks, and every 12 weeks thereafter. **All

laboratory data, including serum levels of ALP, calcium (Ca), and phosphate (P), were

measured in the laboratory of each institute. Abnormal levels of ALP, Ca and P were

based on the age-matched reference range.** Renal ultrasonographic and ophthalmologic

examinations were performed at baseline and every 24 weeks. In patients who had been

already treated by AA outside of this clinical trial, data at the initiation of that treatment were

defined as baseline.

Treatment

All of the patients except one received AA by SC injection three times weekly at a dose of 2

mg/kg and the maximum volume of a single injection was 1 mL (40 or 80 mg/ml

concentration). Patient 004-001, with the adult form, received AA at a dose of 1·17 mg/kg (1

mL SC at a concentration of 80 mg/ml) because that volume was the maximum permitted for

a single injection. The mean ± SD duration of the treatment was 363·6 ± 275·3 days (median

251, range 49–868).

Safety

Adverse events (AEs) including injection-associated reactions and injection site reactions (ISRs) were graded by the investigator as mild, moderate, or severe, and whether or not related to treatment. **ISRs are defined as related AEs that are localized to the area surrounding the injection occurring either during or at any time point after administration of the study drug injection.** Safety was also assessed from change of vital signs and laboratory data, renal ultrasonographic findings, ophthalmologic findings, and drugs used concomitantly during the study. Regarding laboratory data, changes from baseline after treatment were calculated at every visit.

Efficacy

Overall survival was defined as the time from birth to death during the study. Ventilator-free survival for patients who were not mechanically ventilated at the time of enrollment was defined as the percentage of patients who were alive and ventilator-free at the end of the study after treatment.

 Respiratory function in patients with respiratory support was evaluated by ventilator status, time on respiratory support (including time on ventilator or supplemental oxygen), ventilator rate, oxygen volume, ventilator pressures, and fraction of inspired oxygen.

Radiological findings of the wrists and knees were evaluated according to Thacher and colleagues.[15] This scoring method was developed to assess nutritional rickets. Radiographs were evaluated and scored on the rickets severity scale (RSS) every 12 weeks and changes from baseline were calculated.

The effect of AA treatment on physical growth was measured from height, weight, arm span, head circumference, and chest circumference. Height and weight data were transformed to age- and sex-specific z-scores from the average results for the reference Japanese population.[16] Changes of all measurements from baseline were calculated at every visit.

Assessment of changes in gross motor development was based on developmental milestones using a gross motor milestone checklist for this study **(see Supplementary Methods)**. The checklist consisted of four sections assessing each postural position: supine, prone, sitting, and standing. Each section had different numbers of items for gross motor skills: supine ($n = 9$), prone ($n = 10$), sitting ($n = 6$), and standing ($n = 16$). **Examiner checked skills, "yes" or "no" depending on if the patient was able to perform each activity.** The number of skills that had been achieved was scored and totaled.

Statistical analysis

Paired *t*-tests were used to assess changes from baseline in measurements. A *P*-value of <0·05

was considered as significant. Statistical analyses were performed using SAS (version 9.3,

SAS Institute Inc., Cary, NC, USA).

Results

Patient baseline characteristics

Baseline patient characteristics are summarized in Table 1. Thirteen patients (9 females and 4

males) were enrolled in this study. Their median age was 91 days (range 0 days to 34 years).

Ethnically, all were Japanese except for two patients (007-001 and 008-001). The father of

patient 007-001 was American and his mother was Japanese. Patient 008-001 was Chinese.

Ten hospitals each enrolled single patients and one hospital three patients. HPP form was:

perinatal (*n* = 6), infantile (*n* = 5), childhood (*n* = 1), and adult (*n* = 1). **No patients with**

benign pre-natal and odonto form were included. All patients had low levels of serum

ALP at 0–240 IU/l (median 39·0) (see Supplementary Information Table S1 for reference

range). Five of the 13 patients had already been treated with AA prior to this study. Mean

height z-score was –2·5 ± 1·8 SD and mean weight z-score was –1·6 ± 1·5 SD.

The medical history of the patients at baseline is summarized in Table 2. In patients with perinatal and infantile forms, the main symptoms at the onset of HPP were poor weight gain (30·7%), dyspnea (30·7%), and hypomineralization of bone (30·7%). Four patients (30·7%) had family members with HPP. While there were no patients with pseudo-fracture, three patients (23·1%) had a history of bone fractures. Four patients (30·7%) had muscle weakness, and two of these (004-001 and 007-001) had difficulty walking and an unusual gait· Furthermore, patient 004-001 had impaired activities of daily living caused by myalgia and arthralgia. The clinical course of two patients had already been reported before treatment with AA (007-001) or on the compassionate use of AA (003-001) before recruitment into the study.[17,18]

Mean serum Ca was 9·93 ± 0·59 mg/dl, serum P 5·73 ± 1·32 mg/dl, and spot urine calcium/creatinine ratio (Ca/Cr) 0·45 ± 0·50 g/gCr (Supplementary Information Fig. S1). Serum Ca and P levels were within the reference range at baseline (see Supplementary Information Table S2 for reference range). All other laboratory data were normal at baseline.

Safety

A total of 195 AEs was reported: mild 177 (91%), moderate 14 (7%), and severe 4 (2%). Of these, 104 AEs (53%) were assessed by the investigators as related to AA. The most common treatment-related AEs were injection site reactions (total 88 events in 7 patients), which

consisted of mild, localized, and transient erythema that was sometimes associated with induration and pruritus. No generalized injection-associated reactions, including anaphylactic shock or hypotension, were observed in any of the patients (see Supplementary Information Tables S3–S7 for additional AE data).

A total of six serious AEs was reported in two patients (003-001 and 006-001) [Table 3]. Two of these serious AEs (convulsion and hypocalcemia) were possibly related to the treatment in patient 003-001. The convulsion occurred on day 28 and was attributed to hypocalcemia that appeared from day 23. Serum Ca level was improved from 4·7 mg/dl on day 28 to 9·7 mg/dl on day 33 by increasing the dose of Ca administration. No convulsion was observed after the serum Ca level had been stabilized. The other four serious AEs were considered unrelated to treatment. Two of them were associated with infections. **One of 4 serious AEs was mixed deafness in case 003-001.** None of the serious AEs necessitated a change in the doses of the study drug.

Renal ultrasonographic examinations detected nephrocalcinosis (23%) in three patients (001-001, 002-001, and 007-001). These findings were not considered by the investigators as AEs because of the lack of exacerbation during treatment. No patients had ophthalmologic findings, including papilledema and ectopic calcification.

With respect to laboratory data, all measurements except ALP, Ca, and P remained within the normal range (see Supplementary Information Tables S1 and S2 for age-specific reference

ranges for ALP, Ca, and P). For all patients, mean serum ALP level increased rapidly and markedly from 79 ± 86 IU/l at the baseline to $24\ 407 \pm 12\ 701$ IU/l 4 weeks after starting AA treatment. High levels of serum ALP persisted during AA treatment. Serum P levels were transiently or continuously increased above the upper limit of normal (ULN) in 11 patients (84·6%) during treatment. The highest level of serum P (9·7 mg/dl) was observed in patient 003-001 at 4 weeks concomitantly with hypocalcemia (Ca 4·7 mg/dl), as previously described. At a later time point, a high serum P level was also observed in the same patient (8·3 mg/d at 120 weeks). All patients had normal renal function.

In eight patients (61·5%), serum Ca levels were transiently or continuously elevated above the ULN during treatment. The highest serum Ca level during the study was 11·9 mg/dl, observed in patient 009-001 at 16 weeks. In addition, the highest Ca/Cr was observed in patient 001-001 at 8 weeks (3·05 g/gCr), while using a low-calcium formula as additional management for hypercalcemia. Transient or continuous elevations of serum Ca and P levels during AA treatment were observed in three patients (001-001, 005-001, and 008-001). They used low-calcium formula and/or a low-phosphorus formula (see Supplementary Information for details of additional management in these patients).

Efficacy

The survival rate was 100% (95% CI 75·3–100·0) at the end of the study (median 24, range 4–120 weeks).

Five patients (004-001, 005-001, 007-001, 008-001, and 010-001) did not require mechanical respiratory support at baseline nor during the study. Ventilator-free survival among them was 100% at the end of the study (median 24, range 12–60 weeks).

A total of eight patients (61.5%) required some form of respiratory support and three (37·5%) of them were managed with non-invasive respiratory support. Five patients (62·5%) [3 perinatal and 2 infantile form] required invasive mechanical ventilation (IMV) support. Since three perinatal patients had respiratory failure at birth, mainly due to bronchomalacia and hypomineralized ribs, they received IMV support from day 0 and continued after baseline. On the other hand, two infantile patients did not show apparent respiratory failure at birth. However, they had failure to thrive and showed a gradually deteriorating respiratory condition during infancy. At baseline, they had poorly mineralized ribs on radiological findings and received respiratory support (Table 4). Four patients also received tracheostomy to maintain their quality of life during mechanical ventilation support (see Supplementary Information Results for detail).

Respiratory status and mineralization of ribs improved in all patients during AA treatment (see Supplementary Information Results **and Fig. S3** for details). Three patients (37·5%) did

not require respiratory support and two patients were starting to wean off support during the first month of treatment. At the end of the study, one patient was on mechanical ventilation and two received supplementary oxygen, making a total of three patients requiring some form of respiratory support at the end of the study.

Baseline radiographs showed undermineralized metaphyses as hypophosphatasia-associated skeletal lesions in all except two patients with a closed growth plate (004-001 and 007-001). Mineralization gradually improved in all patients. At week 24, these metaphyses were mineralized with distinct provisional zones of calcification, and the metacarpals had wider widths, better-defined cortexes, and no lytic areas at their proximal ends. Mean RSS score decreased during treatment and the changes from the baseline to 12 and 24 weeks were $-3\cdot4 \pm 3\cdot4$ ($P = 0\cdot016$) and $-5\cdot4 \pm 2\cdot7$ ($P = 0\cdot002$), respectively (Fig. 1).

Weight was assessed in all patients and height were evaluated in 11 patients. Height data at baseline were not obtained for two patients who had already been treated with AA prior to this study. Mean weight z-score did not markedly change from $-1\cdot6 \pm 1\cdot5$ SD at the baseline to $-1\cdot6 \pm 1\cdot7$ SD at the end of the study ($P = 0\cdot881$). Mean height z-score, also, did not change significantly from $-2\cdot5 \pm 1\cdot9$ SD at the baseline to $-2\cdot0 \pm 1\cdot4$ SD at the end of the study ($P = 0\cdot139$) [Fig. 2]. Additional data on physical growth are provided in Supplementary Information (Results).

Gross motor milestones were evaluated in 10 patients. Five infants were assessed at

baseline, of whom four were evaluated at 12 weeks. Mean total score for gross motor

milestones was significantly increased at 12 weeks compared to baseline ($P = 0.003$).

Although no baseline data were obtained in five patients who had already been treated with

AA prior to this study, the total score of four infants gradually increased during treatment (see

Supplementary Information Fig. S2).

Discussion

The safety and efficacy of AA have been reported in patients with HPP in international,

multicenter clinical trials, following which SC treatment with AA was approved in several

countries including Japan and the USA.[19] Treatment with the recombinant enzyme is

generally safe, although some AEs have to be carefully monitored. The most frequent AE is a

local reaction to the injection. Hypotensive shock due to anaphylaxis was not observed in our

trial. Our clinical study provides evidence supporting the tolerability of AA treatment at the

recommended dose.

An important AE is hypocalcemia on AA treatment. The recombinant enzyme stimulates

mineralization in bone and this process requires calcium deposition in bone. This may

account for hypocalcemia during treatment. Newborns or infants with HPP sometimes show

hypercalcemia and receive low-calcium formula, which may facilitate the development of

hypocalcemia during AA treatment. We recommend ordinary milk when starting AA

treatment and monitoring serum calcium levels during treatment. Administration of calcium

and vitamin D may be necessary to prevent or resolve hypocalcemia.

Hyperphosphatemia can also be an AE. However, serum phosphate levels were not

particularly high in our study: often less than 8 mg/dl but sometimes over 8 mg/dl up to 9·7

mg/dl. The elevation of serum phosphate levels may aggravate ectopic calcification. Thus,

careful observation is necessary and hyperphosphatemia may require the restriction of

phosphorus intake. While ectopic calcification in the kidney and retina was not observed,

craniosynostosis **that is one of the complications of HPP** occurred in this clinical trial.

These potential AEs should be carefully monitored during treatment. **Mixed deafness was**

considered a serious AE in case 003-001 by doctors who treated the patient.

Sensorineural hearing loss was indicated by auditory brainstem response test, and

conductive deafness was suggested by deformities of the middle ear ossicles detected by

computed tomography. They might be due to their hypomineralization in HPP. In

addition, deafness is reported to be one of clinical features in HPP.[11] Thus, mixed

deafness in this case might be one of the complications in HPP.

Convulsion was observed after the initiation of treatment in one patient. Indeed, vitamin

B6-dependent convulsion is one of the complications of HPP.[1] However, the convulsion in

the patient was due to hypocalcemia. Thus, it is necessary to consider both vitamin B6-

dependent and hypocalcemia-induced convulsions during treatment.

AA clearly stimulated bone formation. Patients with severe HPP showed marked

hypomineralization in all bones, especially the skull, long bones, and ribs. The long bones

and ribs thickened during treatment. The effect was observed at 1 month after starting

treatment. Lung function was improved after bone formation became evident. Thus,

supportive therapy for the respiratory and circulatory functions is essential even after the

initiation of treatment with AA. The survival rate and respiratory function improved in the

trial. Six patients suffered from perinatal HPP, of whom five required mechanical ventilation

and two underwent tracheostomy. **Although AA improved respiratory status, periods to**

the end of respiratory support were different among the patients with perinatal HPP

(Table 4). Patients with high-frequency oscillatory ventilation or synchronized

intermittent mandatory ventilation at baseline required longer respiratory support than

those with nasal continuous positive airway pressure or supplemental oxygen,

suggesting that respiratory status at baseline predicts periods of respiratory support

after the initiation of AA. In agreement with our study, the previous report describes

that severe or long-standing pulmonary impairment at baseline might influence the

improvement period of respiratory status.[12] The six patients with perinatal HPP were all

alive at the final visit (median 48, range 4–120 weeks) and four of them were free from

respiratory support including oxygen supply.

It is strongly suggested that AA treatment of patients with HPP improves prognosis.[13,14]

The treatment has been called transformative.[5] Thus, the early diagnosis of HPP is important

in this situation. A treatment algorithm for HPP has been proposed.[20,21] Other therapies

including teriparatide, bone marrow transplantation, and gene induction have been

reported.[22–24] We hope to develop a guide on how to manage patients with HPP in terms of

diagnosis and treatment in the near future. In summary, asfotase alfa was safe and effective

for the treatment of 13 patients with HPP including perinatal and childhood forms.

References

1)   Whyte, M.P. (2016) Hypophosphatasia: aetiology, nosology, pathogenesis, diagnosis

     and treatment. *Nature Reviews Endocrinology*, **12**, 233–246.

2)   Millán, J.L. & Whyte, M.P. (2016) Alkaline phosphatase and hypophosphatasia.

     Calcified Tissue International, **98**, 398–416.

3)   Ozono, K., Yamagata, M., Michigami, T., *et al*. (1996) Identification of novel missense

     mutations (Phe310Leu and Gly439Arg) in a neonatal case of hypophosphatasia.

     Journal of Clinical Endocrinology and Metabolism, **81**, 4458–4461.

4) Wenkert, D., McAlister, W.H., Coburn, S.P., *et al*. (2011) Hypophosphatasia: nonlethal

disease despite skeletal presentation in utero (17 new cases and literature review).

Journal of Bone and Mineral Research, **26**, 2389–2398.

5) Bishop, N., Munns, C.F. & Ozono, K. (2016) Transformative therapy in

hypophosphatasia. *Archives of Disease in Childhood*, **101**, 514–515.

6) Linglart, A. & Biosse-Duplan, M. (2016) Hypophosphatasia. *Current Osteoporosis*

Reports, **14**, 95–105.

7) Whyte, M.P., Zhang, F., Wenkert, D., *et al*. (2015) Hypophosphatasia: validation and

expansion of the clinical nosology for children from 25 years experience with 173

pediatric patients. *Bone*, **75**, 229–239.

8) Michigami, T., Uchihashi, T., Suzuki, A., *et al*. (2005) Common mutations F310L and

T1559del in the tissue-nonspecific alkaline phosphatase gene are related to distinct

phenotypes in Japanese patients with hypophosphatasia. *European Journal of*

Pediatrics, **164**, 277–282.

9) Watanabe, A., Karasugi, T., Sawai, H., *et al*. (2011) Prevalence of c.1559delT in ALPL,

a common mutation resulting in the perinatal (lethal) form of hypophosphatasia in

Japanese and effects of the mutation on heterozygous carriers. *Journal of Human*

Genetics, **56**, 166–168.

10) Ozono, K. & Michigami, T. (2011) Hypophosphatasia now draws more attention of both clinicians and researchers: a commentary on prevalence of c.1559delT in ALPL, a common mutation resulting in the perinatal (lethal) form of hypophosphatasias in Japanese and effects of the mutation on heterozygous carriers. *Journal of Human Genetics*, **56**, 174–176.

11) Taketani, T., Onigata, K., Kobayashi, H., *et al*. (2014) Clinical and genetic aspects of hypophosphatasia in Japanese patients. *Archives of Disease in Childhood*, **99**, 211–215.

12) Whyte, M.P., Rockman-Greenberg, C., Ozono, K., *et al*. (2016) Asfotase alfa treatment improves survival for perinatal and infantile hypophosphatasia. *Journal of Clinical Endocrinology and Metabolism*, **101**, 334–342.

13) Whyte, M.P., Greenberg, C.R., Salman, N.J., *et al*. (2012) Enzyme-replacement therapy in life-threatening hypophosphatasia. *New England Journal of Medicine*, **366**, 904–913.

14) Whyte, M.P., Madson, K.L., Phillips, D., *et al*. (2016) Asfotase alfa therapy for children with hypophosphatasia. *JCI Insight*, **1**, e85971.

15) Thacher, T.D., Fischer, P.R., Pettifor, J.M., *et al*. (2000) Radiographic scoring method for the assessment of the severity of nutritional rickets. *Journal of Tropical Pediatrics*, **46**, 132–139.

16) Ito, Y., Kato, N., Tachibana, K., *et al*. (2005) "Standard height" and "standard growth curve" 2000 version conform to the standardized height in Treatment Support Program

for the Chronic Pediatric Diseases of Specified Categories. *The Journal of Pediatric Practice*, **68**, 1343–1351.

17) Mochizuki, H., Saito, M., Michigami, T., *et al.* (2000) Severe hypercalcaemia and respiratory insufficiency associated with infantile hypophosphatasia caused by two novel mutations of the tissue-nonspecific alkaline phosphatase gene. *European Journal of Pediatrics*, **159**, 375–379.

18) Okazaki, Y., Kitajima, H., Mochizuki, N., *et al.* (2016) Lethal hypophosphatasia successfully treated with enzyme replacement from day 1 after birth. *European Journal of Pediatrics*, **175**, 433–437.

19) Scott, L.J. (2016) Asfotase alfa in perinatal/infantile-onset and juvenile-onset hypophosphatasia: a guide to its use in the USA. *BioDrugs*, **30**, 41–48.

20) Saraff, V., Narayanan, V.K., Lawson, A.J., *et al.* (2016) A diagnostic algorithm for children with low alkaline phosphatase activities: lessons learned from laboratory screening for hypophosphatasia. *Journal of Pediatrics*, **172**, 181–186.

21) Taillandier, A., Domingues, C., De Cazanove, C., et al. (2015) Molecular diagnosis of hypophosphatasia and differential diagnosis by targeted next generation sequencing. *Molecular Genetics and Metabolism*, **116**, 215–220.

22) Whyte, M.P., Mumm, S. & Deal C. (2007) Adult hypophosphatasia treated with teriparatide. *The Journal of Clinical Endocrinology and Metabolism*, **92**, 1203–1208.

23) Iijima, O., Miyake, K., Watanabe, A., *et al*. (2015) Prevention of lethal murine hypophosphatasia by neonatal *ex vivo* gene therapy using lentivirally transduced bone marrow cells. *Human Gene Therapy*, **26**, 801–812.

24) Sugano, H., Matsumoto, T., Miyake, K., *et al*. (2012) Successful gene therapy *in utero* for lethal murine hypophosphatasia. *Human Gene Therapy*, **23**, 399–406.

Figure legends

Fig. 1 A) Change of rickets severity scale (RSS) score during treatment. Mean RSS score decreased from $8·0 ± 2·9$ at baseline to $4·9 ± 3·8$ at 12 weeks ($n = 10$) and $3·0 ± 2·8$ at 24 weeks ($n = 9$). **B) Change of the wrist and knee radiographs during treatment. Patient 011-001, with the perinatal form, is shown. Undermineralized methaphyses were improved at week 12. RSS, Rickets Severity Score.**

Fig. 2 Change in (A) height and (B) weight z-scores during treatment. Mean weight z-score did not markedly changed from $−1·6 ± 1·5$ SD at baseline to $−1·6 ± 1·7$ SD at the end of the study ($P = 0·881$). Mean height z-score did not change significantly from $−2·5 ± 1·9$ SD at baseline to $−2·0 ± 1·4$ SD at the end of the study ($P = 0·139$).

Table 1. Baseline patient characteristics

Case no.	Sex	Age	HPP form	Mutations of *ALPL*	ALP (U/l)*	Height z-score (cm)	Weight z-score (kg)	Final visit (week)
001-001	F	113 days	I	p.M295I/c.1559delT	70	51·0 (–4·1)	4·25 (–2·4)	36
002-001	F	230 days	I	p.H336R/c.1559delT	21	61·0 (–2·8)	4·80 (–4·2)	120
002-002	M	16 days	P	c.1559delT/c.1559delT	23	51·0 (1·0)	2·89 (–0·3)	84
002-003	F	0 days	P	c.1559delT/c.1559delT	0	41·0 (–3·6)	2·43 (–1·2)	4
003-001	F	1 day	P	p.G491R/p.G491R	1	42·8 (–2·7)	2·68 (–0·6)	120
004-001	M	34 years	A	c.1559delT heterozygous	51	159·4 (–2·3)	68·6 (–0·0)	24
005-001	F	158 days	I	p.E191G/c.1559delT	144	57·0 (–3·4)	6·06 (–1·1)	24
006-001	F	54 days	P	c.1559delT/c.1559delT	15	46·6 (–2·8)	2·93 (–2·3)	24
007-001	M	17 years	I	p.K224E/p.G426C	195	148·8 (–3·7)	40·0 (–3·9)	24
008-001†	F	36 days	I	p.R136C/p.F327L	240	57·0 (2·1)	4·70 (0·9)	60
009-001	F	0 days	P	p.R450C/c.1559delT	39	41·0 (–3·6)	2·30 (–1·6)	72
010-001	M	10 years	C	p.F327L/p.G339R	209	119·2 (-3·1)	24·4 (–1·7)	12
011-001	F	91 days	P	c.1559delT/c.1559delT	23	52·0 (–3·6)	4·68 (–1·7)	12

A, adult; ALP, alkaline phosphatase; C, childhood; F, female; HPP, hypophosphatemia; I, infantile; M, male; P, perinatal.

* Reference range at 0–1 months: 530–1620 U/l.

†Height measured at 3 days after the baseline.

Table 2. Baseline patient medical history

Case no.	HPP form	Age at onset	Symptoms at HPP onset	Family members with HPP	Fracture history (age detected)	Orthopedic findings	Respiratory status	Serum calcium and phosphate levels, and nephrocalcinosis
001-001	I	2m	Poor weight gain (poor feeding)	Elder brother*	Rib (at infancy)	Chest deformity, cranial deformity	Pneumonia	Nephrocalcinosis, hypercalcemia
002-001	I	1m	Poor weight gain			Chest deformity, cranial deformity, muscle weakness	Dyspnea	Nephrocalcinosis, hypercalcemia
002-002	P	0m	Seizure, dyspnea, hypercalcemia, hyperphosphatemia				Dyspnea	Hypercalcemia, hyperphosphatemia
002-003	P	0m	Chest deformity, dyspnea, short extremities	Elder brother (002-002)			Dyspnea	
003-001	P	0m	Hypomineralization of bone (pre-natal)			Chest deformity	Dyspnea	
004-001†	A	24y	Muscle pain, muscle weakness	Child	Rt. humerus (6y) Lt. clavicle (23y)	Gait disturbance, arthralgia		

ID							
005-001	I	0m	Bowed legs		Genu varum, forearm curvature		Hypercalcemia
006-001	P	0m	Short extremities, hypomineralization of bone, chest deformity, dyspnea	Lt. radius (1m) Rt. ulna (1m)	Genu varum, muscle weakness	Dyspnea, pneumonia	
007-001‡	I	2m	Poor weight gain, bad mood		Delayed walking, chest deformity, cranial deformity, bone pain, arthralgia, gait disturbance, muscle weakness	Dyspnea, pneumonia	Nephrocalcinosis, hypercalcemia
008-001	I	0m	Hypomineralization of bones (metaphyseal flaring)				Hyperphosphatemia
009-001	P	0m	Short extremities, hypomineralization of bones		Genu varum		
010-001	C	3y	Premature tooth loss		Gait disturbance, arthralgia		
011-001	P	1m	Dyspnea, poor weight			Dyspnea	Hypercalcemia

gain

A, adult; C, childhood; HPP, hypophosphatasia; I, infantile; Lt, left; m, month; P, perinatal; Rt, right; y, year

*Brother of 001-001, died of respiratory dysfunction from pneumonia at the age of 3 months, diagnosed with HPP by genetic testing.

†Patient 004-001 had internal plate fixation of humerus fracture and muscle biopsy for muscle weakness.

‡Patient 007-001 underwent surgery for craniosynostosis at the age of 1 year.

Table 3. Serious adverse events

Case no.	Age at AE onset	Preferred term	Severity	Causality	Outcome	AE duration
003-001	28 days	Convulsion	Severe	Probable	Resolved	16 days
	23 days	Hypocalcemia	Severe	Probable	Resolved	21 days
	7·7 months	Mixed deafness*	Severe	Unrelated	Unresolved	
	1·3 years	Upper respiratory tract infection†	Moderate	Unrelated	Resolved	5 days
006-001	3·4 months	Staphylococcal infection‡	Severe	Unrelated	Resolved	20 days
	5·3 months	Convulsion§	Moderate	Unrelated	Resolved	2 days

AE, adverse event.

*Mixed deafness was based on auditory brainstem response. Deformities of the middle ear ossicles were detected using computed tomography.

†Upper respiratory tract infection resolved by intravenous fluid therapy for 5 days while hospitalized.

‡Staphylococcal infection caused by catheter infection and cured by antibacterial therapy.

§Convulsion was a withdrawal symptom from benzodiazepine given for sedation during respiratory management.
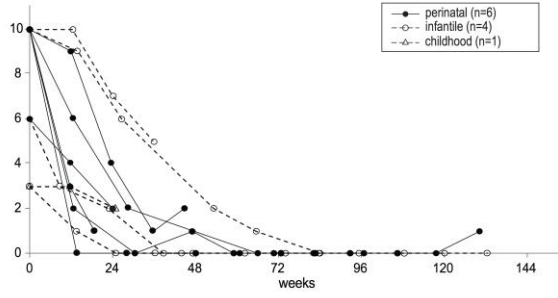
Table 4. Respiratory support

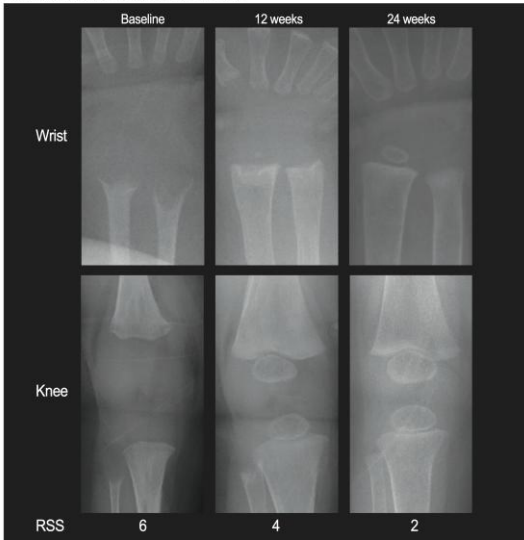| Case no.	HPP form	Respiratory status at the baseline	Period from baseline to weaning off mechanical ventilation	Period from baseline to the end of respiratory support*
001-001	I	SIMV (started at 8 days before baseline)	121 days (tracheostomy at 9 days from baseline: SIMV for 23 days and CPAP for 98 days.)	Ongoing supplemental oxygen at the final visit (36 weeks)
002-001	I	BiPAP (SIMV for 32 days before BiPAP)	205 days	272 days
002-002	P	Nasal CPAP	No mechanical ventilation support	23 days
002-003	P	Nasal CPAP	No mechanical ventilation support	34 days (nasal CPAP for 3 days and nasal high flow for 31 days)
003-001	P	HFO (with inhaled nitric oxide)	225 days (tracheostomy at 78 days from baseline. HFO control for 108 days; SIMV for 7 days and then gradually tapered)	1·8 years
006-001	P	HFO	110 days (tracheostomy at 90 days from baseline. HFO control for 35 days; A/C mode for 51 days and then SIMV control.)	Ongoing supplemental oxygen at the final visit (24 weeks)
009-001	P	Supplemental oxygen	No mechanical ventilation support	3 days
011-001	P	SIMV (tracheostomy at 14 days before baseline)	Ongoing SIMV control	Ongoing SIMV control at the final visit (12 weeks)

A/C, assist control ventilation; BiPAP, biphasic positive airway pressure; CPAP, continuous positive airway pressure; HFO, high-frequency oscillatory ventilation; I, infantile; P, perinatal; SIMV, synchronized intermittent mandatory ventilation.

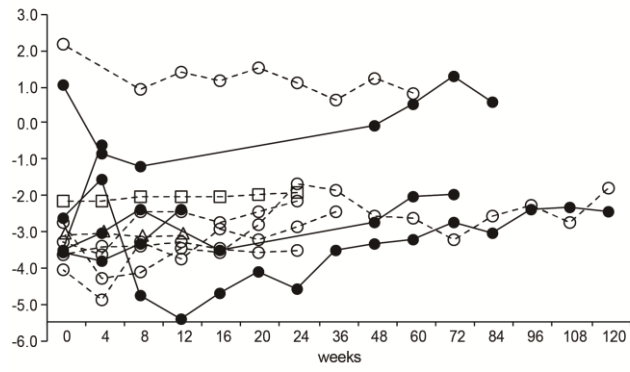*Respiratory support including oxygen supply.
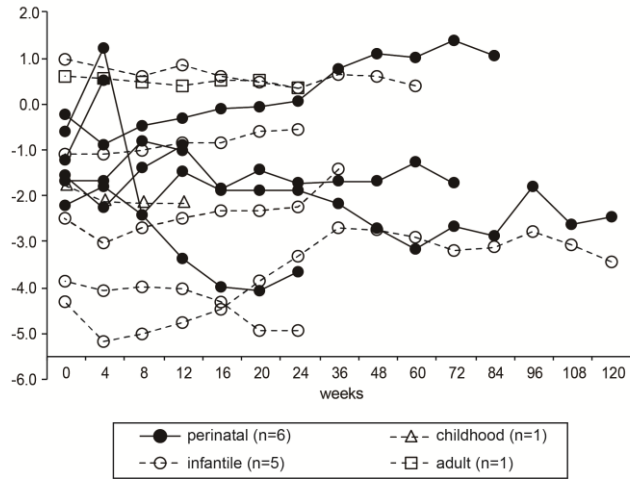
A. Rickets severity scale

B. Representative radiographic change

A. Height SD score

B. Weight SD score

| perinatal (n=6) | childhood (n=1) |
| infantile (n=5) | adult (n=1) |

CrossMark

ORIGINAL ARTICLE

Characteristic calcaneal ossification: an additional early radiographic finding in infants with fibrodysplasia ossificans progressiva

Sachi Hasegawa[1] · Teresa Victoria[2] · Hülya Kayserili[3] · Elaine Zackai[4] ·
Gen Nishimura[5] · Nobuhiko Haga[5] · Yasuharu Nakashima[5] · Osamu Miyazaki[5] ·
Hiroshi Kitoh[1,5]

Abstract
Background We have clinically encountered children with fibrodysplasia ossificans progressiva who had abnormal calcaneal ossification.
Objective To evaluate whether calcaneal ossification variants are significant radiographic findings in children with fibrodysplasia ossificans progressiva.
Materials and methods Lateral feet radiographs in nine children who fulfilled the diagnostic criteria of fibrodysplasia ossificans progressiva were reviewed. The studies were obtained during infancy or early childhood.
Results Fourteen lateral foot radiographs of fibrodysplasia ossificans progressiva were available for this study (ages at examination: 1-104 months). Four children ages 2 months to 11 months showed double calcaneal ossification centers; 7 children had plantar calcaneal spurs that decreased in size with age. Overall, eight of nine children with fibrodysplasia ossificans progressiva demonstrated double calcaneal ossifications and/or plantar calcaneal spurs in infancy or childhood.
Conclusion Double calcaneal ossification centers in early infancy and plantar calcaneal spurs in childhood are frequently seen in children with fibrodysplasia ossificans progressiva and may be a useful radiologic indicator for early diagnosis.

Keywords Calcaneal spur · Children · Double calcaneal ossification center · Early diagnosis · Fibrodysplasia ossificans progressiva · Radiography

✉ Hiroshi Kitoh
hkitoh@med.nagoya-u.ac.jp

1 Department of Orthopaedic Surgery,
Nagoya University Graduate School of Medicine,
65 Tsurumai, Showa-ku, Nagoya, Aichi 466-8550, Japan

2 Department of Radiology, Children's Hospital of Philadelphia,
Philadelphia, PA, USA

3 Medical Genetics Department,
Koç University School of Medicine (KUSOM),
İstanbul, Turkey

4 Department of Medical Genetics,
Children's Hospital of Philadelphia,
Philadelphia, PA, USA

5 The Research Committee on Fibrodysplasia Ossificans Progressiva,
Tokyo, Japan

Introduction

Fibrodysplasia ossificans progressiva is a genetic disorder of the connective tissues caused by activating mutations in the gene-encoding activin receptor IA/activin-like kinase 2 (ACVR1/ALK2), a bone morphogenetic protein (BMP) type I receptor [1]. Most affected individuals have a common mutation (c.617G > A, p.R206H). The clinical hallmark of fibrodysplasia ossificans progressiva is progressive heterotopic ossification of soft tissues, such as muscles, ligaments, tendons, fasciae and aponeuroses, which causes significant physical morbidity and may lead to early mortality. Traumatic injury and surgical intervention induce explosive heterotopic ossification in patients with fibrodysplasia ossificans progressiva. Early diagnosis is necessary to prevent additional trauma or iatrogenic harm [2].

Fibrodysplasia ossificans progressiva is associated with a variety of bone malformations as well as variant ossification. Awareness of the bone anomalies may facilitate prompt diagnosis. Malformations of the great toes are well-known and are the most prevalent indicators of this disorder [3]. Other anomalies include shortening of the first metacarpal bones and

hypertrophy of the posterior element of the cervical spine [4]. Quantitative analyses of bone changes in the hand and cervical spine are also available [5]. Recently, we encountered two children with distinctive double ossification centers and plantar spurs in the calcaneus. Search of the database identified seven additional children with fibrodysplasia ossificans progressiva. We evaluate whether the presence of calcaneal changes may be commonly seen in patients with fibrodysplasia ossificans progressiva.

Materials and methods

Two children (cases 2 and 3 in Table 1) were seen clinically and subsequently presented and discussed in web case consultations. The online discussion enabled us to collect clinical data and foot radiographs from members of the Research Committee on Fibrodysplasia Ossificans Progressiva (Japan), who provide pediatric orthopedic services in four hospitals across Japan. Six Japanese children and one Indian child (5 males and 2 females) who underwent lateral feet radiography in infancy or early childhood were thus additionally enrolled. All nine children fulfilled the diagnostic criteria of fibrodysplasia ossificans progressiva, including deformities of the great toes, extraskeletal heterotrophic ossification, joint contractures, fusion of the cervical spine, broad femoral necks and osteochondroma-like lesions. Seven of the nine children underwent molecular testing, showing the common ACVR1/ALK2 mutation within the glycine/serine-rich regulatory (GS) domain (c.617G > A, p.R206H). All radiographs were examined by a single reader (G.N.) with 30 years' clinical experience in the field of skeletal dysplasias and specifically focused on calcaneal configurations.

Results

Fourteen lateral foot radiographs obtained between the ages of 1 month to 104 months were available for this study. Three children (cases 1, 2 and 4) underwent serial radiographic examinations in infancy and early childhood. We found two distinctive findings: 1) double calcaneal ossification centers and 2) plantar calcaneal spurs. These findings were bilateral and symmetrical. The radiologic findings and pertaining clinical information are summarized in Table 1.

Double calcaneal ossification centers

Four children (cases 1, 2, 3 and 4) showed double ossification centers in radiographs obtained in infancy (Figs. 1, 2, 3 and 4). Three of them (cases 2, 3 and 4) had a cleft separating the anterior two-thirds from the posterior third in the calcaneus. The posterior ossification centers were small, intermediate and large in size at ages 2, 4 and 10 months, respectively, partially fused with the anterior ossification centers at ages 4 and 10 months, and completely incorporated into the anterior ossifications at ages 12 months and 22 months. The remaining child (case 1) had a cleft separating the anterior third from the posterior two-thirds in the calcaneus. The anterior ossification center manifested as punctate multiple ossifications in early infancy, which evolved into double ossifications at age 11 months and completely coalesced at age 3 years.

Plantar calcaneal spur

Seven children showed a small spur from the plantar aspect of the posterior calcaneal body (Figs. 2, 3, 4 and 5). The spurs are pedunculated and projected posteriorly from the posterior

Table 1 Demographic, clinical, genetic and radiologic summaries of nine children with fibrodysplasia ossificans progressive

Case number	1				2		3	4		5	6	7	8	9
Sex	male				male		female	male		male	female	male	male	female
Current age	4Y8M				6Y		2Y9M	3Y2M		2Y	3Y5M	4Y6M	7Y7M	8Y8M
Ethnic background	Japanese				Caucasian		Turkish	Japanese		Indian	Japanese	Japanese	Japanese	Japanese
ACVR1 mutation	R206H				R206H		ND	R206H		R206H	ND	R206H	R206H	R206H
Great toe abnormalities	+				+		+	+		+	+	+	+	+
Other radiological findings of FOP	+				NA		NA	+		+	+	+	+	+
Ectopic ossification	+				-		-	-		-	-	-	+	+
Age at X-ray (months)	1	3	11	36	2	12	4	10	22	15	18	33	70	104
Double calcaneal ossification centers	punctate	punctate	+	-	+	-	+	+	-	-	-	-	-	-
Plantar calcaneal spur	-	-	-	-	+	+	+	+	+	+	-	+	+	+

NA not available , *ND* not determined